Hard Coatings with High Temperature Adaptive Lubrication and Contact Thermal Management: Review of Recent Progress

A.A. Voevodin, C. Muratore, S.M. Aouadi

PII: S0257-8972(14)00376-4
DOI: doi: 10.1016/j.surfcoat.2014.04.046
Reference: SCT 19366

To appear in: *Surface & Coatings Technology*

Received date: 9 January 2014
Revised date: 17 April 2014
Accepted date: 18 April 2014

Please cite this article as: A.A. Voevodin, C. Muratore, S.M. Aouadi, Hard Coatings with High Temperature Adaptive Lubrication and Contact Thermal Management: Review of Recent Progress, *Surface & Coatings Technology* (2014), doi: 10.1016/j.surfcoat.2014.04.046

Submitted for publication in Surface and Coatings Technology

Hard Coatings with High Temperature Adaptive Lubrication and Contact Thermal Management: Review of Recent Progress

A.A.Voevodin[1], C. Muratore[2], S.M.Aouadi[3]*

[1]*Materials and Manufacturing Directorate, Air Force Research Laboratory, Wright-Patterson Air Force Base, OH 45433, USA*

[2]*Department of Chemical and Materials Engineering, University of Dayton, Dayton, OH 45469, USA*

[3]*Department of Materials Science and Engineering, University of North Texas, Denton, TX 76207, USA*

Abstract

Progress in the design and exploration of hard coatings with high temperature adaptive behavior in tribological contacts is reviewed. When coupled with most recent surface engineering strategies for high temperature contact thermal management, this progress opens a huge opportunity for adaptive coating applications on machine parts, where oils and coolants are commonly used. The adaptive mechanisms discussed here include metal diffusion and formation of lubricant phases at worn surfaces, thermally- and mechanically-induced phase transitions in hexagonal solids, contact surface tribo-chemical evolutions to form phases with low melting point, formation of easy to shear solid oxides, and others. All of these adaptive mechanisms are combined in nanocomposite coatings with synergistic self-adaptation of surface structure and chemistry to lubricate from ambient temperatures to 1000 °C and provide surface chemical and structural reversibility during temperature cycling to maintain low friction coefficients. The review also highlights emerging surface adaptive concepts, where advances with *ab initio* modeling of intrinsically layered solids point to new compositions for thermally stable, easy to shear ceramic coatings, load- and temperature-adaptive surfaces with arrays of compliant carbon and boron nitride nanotubes as well as low friction two-dimensional structures. Approaches for self-regulation of coating thermal conductivity, heat flow, and thermal spike mitigations are discussed in the context of surface structure evolution and phase transitions. Future progress is linked to the development of *in situ* exploration techniques, capable of identifying adaptive surface chemistry and structural evolutions in broad temperature regimes. When combined with predictive modeling, such approaches drastically accelerate adaptive coating developments. The review identifies opportunities, strategies, and challenges for designs and applications of hard coatings with high temperature adaptive lubrication and contact thermal management.

Key words: hard coating; high temperature; solid lubrication; thermal management; adaptive; tribology

***** Corresponding author – andrey.voevodin@us.af.mil; +1-937-255-4651 phone; +1-937-255-2176 fax

Submitted for publication in Surface and Coatings Technology

Highlights

- Hard coating adaptive lubrication for up to 1000 °C and temperature cycling.
- Self-regulation of thermal conductivity, heat flow, and thermal spike mitigation.
- Intrinsically layered thermal stable and easy to shear coatings.
- Adaptive surface perspectives with nanotube arrays and 2D materials.
- *In situ* techniques for tracking high temperature phase and structural evolutions.

1. Introduction

Surface friction and wear reduction remain as acute technological challenges from prehistoric times to modern days. Traditionally, the lubrication of machinery components was driven mainly by improving energy transmission efficiencies with reduced coefficient of friction (CoF) and increasing component life spans with reduced wear rates. From such a perspective, oils and other liquid lubricants are now dominating the field of machine part lubrication. However, recent attention to pollution prevention and weight minimization of transportation mechanisms has accelerated incentives for the advancement of solid lubrication to replace, where possible, oils and their circulation systems. The challenge is not only to develop hard solid lubricated coatings which can reliably maintain low contact friction and wear rates, but to also address thermal management issues of sliding and rolling contacts. In the most practical cases, oils are used both as lubricants and coolants. By advancing both lubrication and thermal management functions of hard coatings, there are multiple opportunities for the expansion of their application, where current oil lubrication market is estimated at $18.7bn in the USA alone [1].

One successful example of a lubrication technology paradigm shift from liquid to solid materials is the recent transition of cutting and milling operations to dry machining, which was dictated by environmental protection requirements and elimination of costs for coolant media recirculation and utilization. This paradigm shift in machining technology was supported by developments of thermally stable high temperature tool materials with hard and wear resistant surfaces. This first started with nitride and carbide based monolithic and multilayered coatings with structure, architecture, and processing all optimized to achieve peak hardness [2-6]. In recent years, these materials evolved into modern day composite hard coatings with complex chemistry and compositions for optimized hardness, toughness, and high temperature stability, where several reviews can be found in the literature [7-15]. Tool coating developers understood the importance of high temperature oxidation protection from the beginning, resulting in the introduction of Al, Cr, Si, B and other oxide and nitride forming elements to the hard coating compositions to form oxidation protective surface layers. For example, single phase TiN coatings, which structure control with ion bombardment was thoroughly studied by Petrov et al. [3], have evolved into a broad spectrum of oxidation resistant hard coatings where TiN is the primary component, including TiAlN, TiAlCrN, TiAlBN, TiAlSiN, TiAlBSiN, TiN-Si_3N_4, TiN-TiB_2 and other examples [9,16-24]. Most recent advancements in tool coatings are targeting friction reduction in the cutting zone to reduce energy consumption during machining operations. The development of tool coatings with adaptive capability to form high temperature lubricating vanadium, molybdenum, and other Magnéli phase oxides [25] is one of the ongoing efforts in tool coating research [12,26-29].

The example of hard coating successes enabling dry machining operations clearly demonstrates the benefits of solid lubrication for energy and costs savings. There is still more work to be carried out to expand high temperature solid lubrication to general energy dissipating mechanical contacts (bearings, gears, rails, etc.). At this time, the practice of solid lubricants for machine components is mostly limited to temperatures when contact oxidation and structure evolution processes are minimized (e.g. ambient or space). Solid lubricant material systems and approaches for forming easy-to-shear films in the contacts are well reviewed in the literature [30-36]. They are typically integrated with load bearing engineered surfaces, which common designs and selections can be found in a review by Matthews et al. [37]. The most widely used solid lubricants for ambient conditions are based on transition metal dichalcogenides,

graphite, diamond-like carbon, and fluoride polymers. All of these are subject to severe oxidation and deterioration at above 300 °C in air, while we note that hard tool coatings can operate well above that temperature at the contact zone. To better adapt lessons from hard coating designs for tools, we highlight several practically important strategy-differentiating factors in developing high temperature solid lubricants for machines from that of the tool coatings. First is the hardness requirement: while for tools this is a prime metric to ensure reliable cutting, tool life time, and machining quality, the machine contacts do not normally require very hard mating contacts as the contact load is usually distributed and contact fatigue is better avoided with contact surface compliance. Second is the environmental robustness: most machines have interrupted operations, which add both regular and irregular temperature oscillations as well as corrosive and oxidative exposures of various length. Third is the requirement for stable operation: machine drive trains are designed for specific energy losses and the stability of the friction loss in their contacts is critical for reliable and predicted operation over the broad variations of loads, speeds, temperatures and environments.

Driven by stringent system weight reduction requirements, aerospace development and research centers were consistently investing in the exploration and development of high temperature solid lubrication. Application examples include lubrication of hybrid and airfoil bearings of jet engines, splines and bushings of jet and rocket thrust vector controls, mechanisms for flight control surfaces of high Mach planes and space-to-air re-entry vehicles. One of the most successful high temperature lubrication systems was realized by USA National Aeronautics and Space Administration laboratories when using plasma spray composites for superalloy surface lubrication. In this approach, a Ni-Cr coating base was enhanced with hard and temperature stable chrome oxide as well as with additions of silver and low melting point barium and calcium fluoride eutectics to provide broad temperature lubrication [38-41]. One of the best performing coating compositions, designed as PS304, consists of 20 wt.% of Cr_2O_3, 10 wt.% of silver and 10 wt.% of fluorides added to a Ni-Cr base, which was successfully demonstrated with foil gas bearings and other high temperature sliding contacts [42,43]. In parallel to plasma spray technologies, there is a continued interest in thin film methods for the adaptive coating preparations. Researchers at USA Air Force Research Laboratories and their co-workers have synthesized and evaluated a number of broad temperature compositions with physical vapor deposition methods, where initial multiphase adaptive oxide and fluoride coatings for high temperature lubrication [44-48] were progressively evolved to hard oxide matrices with additions of easy to shear gold and silver for moderate temperatures [49-54] and dichalcogenide and carbon phases for near room temperature lubrication [55-57]. These were most recently extended to include lubricious oxide forming nitride matrices to encapsulate low temperature lubricating components [58-62]. There are also recent advances in nanoscale engineered materials with the potential for easy shear at moderate to high temperatures, such as carbon nanotube based composite lubricants [63], intrinsically layered ceramic phases [64-66], graphene [67] and other two-dimensional (2D) low friction hexagonal materials, which may be adapted to thin film technology. While these works showed both possibilities and initial successes of the high temperature solid lubrication and wear protection for machine components, they also identified multiple challenges to be addressed.

In addition to a stable operation at elevated temperatures, most of the mechanical contacts can experience a cold start followed by rapid heating or low/high temperature cycling during the operation. This dictates a need for the hard solid lubricated surfaces for which the CoF can be stable over the broad temperature range and during temperature cycling. Over the last decade, there was a significant progress in adaptive

thin film surface modifications, where contact strain, environment, and temperature are used to trigger evolutions of material surface chemistry and structure to provide low friction and wear in a broad range of operating environments [68-70], temperatures [34,51,55,56,60], and contact loads [69,71,72]. In some of these works, an analogy with the protective skin of a chameleon was used to highlight the intention of a reversible surface adaptation to follow environment changes or temperature cycles. A schematic of a 'chameleon' tribological surface adaptive behavior is shown in Figure 1, which incorporates adaptation to both ambient humidity and temperature [73]. There are several review articles, which discuss chameleon adaptive solid lubrication [31,33,34,69] and also point out that the high temperature adaptive behavior is the most complex and challenging.

To specifically address high temperature adaptive behavior for hard tribological coatings, this review is focused on current and possible future strategies for solid lubrication and thermal management of hard coatings, where temperature oscillations from room to over 500 °C and, in some cases, up to approximately 1000 °C can be sustained in oxidative environments. For such operations, contact softening, melting, and oxidation all need to be synergistically addressed to avoid their detrimental effects on the lubrication mechanisms. Emerging approaches with easy to shear nanolaminated ceramic coatings, compliant composite coatings made with nanotube matrices, and 2D low friction materials are also discussed for temperature and load adaptive tribological contacts. A special attention is given to adaptive thermal management of sliding contacts with solid lubrication, where structure and phase evolutions of composite coatings is used to regulate contact heat flow at elevated temperatures. The review is limited to thin film technologies, where the thickness of the overall coating is of the order of a few microns or less and hence can be used as a finishing operation for the machine part manufacturing.

2. High temperature lubrication adaptive mechanisms

Temperature adaptive chameleon behavior is schematically depicted in the left side of the Figure 1 and involves complex chemical-physical-structural evolution of the contact surfaces. These evolutions are self-guided toward formation of low friction and wear contact conditions for effective adaptive behavior. Over the most recent years several main strategies were applied to achieve such:

i) temperature activated diffusion of metal lubricants to the surface;
ii) temperature and environment activated formation of lubricious oxide phases;
iii) temperature and strain actuated structural evolutions in the contact.

Table 1 compares temperature ranges achieved with each of the above mechanisms and summarizes the benefits and challenges of these strategies. As can be seen from the table, neither of the mechanisms can cover the entire temperature range from room to the order of 1000 °C in air, which creates a challenge for their use in lubricating machine components. However, a combination of these mechanisms can cover the full range and provide reversibility, i.e. both low-to-high and high-to-low temperature adaptive behavior. Examples of the realization for each of the identified mechanisms are discussed in more detail in the sections below together with directions for synergistic combinations of these mechanisms.

2.1. Adaptive mechanisms using metal diffusion

2.1.1. Noble metals as solid lubricants for hard coatings

Silver and gold are reliable solid lubricants used for applications in air and vacuum [74]. They exhibit low shear strength over a range of temperatures spanning from below ambient to their melting points and function best when applied to a hard supporting substrate [75,76]. Their CoF is sensitive to the thickness of the soft metal layer, with the lowest friction observed at thicknesses in the 300-1000 nm range [76,77]. For thinner films, full surface coverage of the substrate is not achieved in the wear track, while for thicker films, a larger share of the load capacity is carried by the soft metallic film resulting in a significant "plowing force" and increasing the total tangential force [78]. Room-temperature friction coefficients between 0.2 and 0.4 are typical for noble metal coatings against steel counterparts within the optimum thickness range [77]. One common drawback of metal lubricants is their low wear resistance at elevated temperatures, when they are softened and easily extruded out of the wear tracks.

Hard nanocomposite coatings were developed to take advantage of the solid lubrication with noble metals outlined above while maintaining wear resistance. Binary yttrium stabilized zirconia (YSZ) and gold nanocomposite coating materials demonstrated high hardness (~15 GPa) with up to 20 atomic percent (at.%) of Au addition [79]. Coatings with 10-20 at.% Au exhibited high ductility and fracture resistance. When YSZ-Au coatings in this compositional range were heated to temperatures of 500 °C, microscopic grains of Au were observed via electron microscopy on the surface, providing a low-shear interface on a hard surface capable of supporting the applied contact load and a reduced CoF [49]. These films provided friction coefficients of approximately 0.2-0.4 from room temperature to 500 °C during sliding in air against a sapphire counterpart. This is consistent with noble-metal lubricant friction performance on hard substrates. Studies of YSZ-Au composite coating structure after high temperature testing revealed that nanoscopic volumes of noble metals spontaneously coalesce at the coating surface to allow the macroscopic lubrication. Other studies of noble-metal nano-crystalline inclusions embedded in ceramic matrices followed, including TiC-Ag [80], YSZ-Ag [50,51], Ta_2/Cr_2AlC-Ag [64], CrN-Ag [81-83], CrAlN-Ag [84], Mo_2N-Ag [85], and MoCN-Ag [86]. These studies of Ag-lubricated hard coatings demonstrated friction coefficients between 0.2 and 0.4 for 10-20 at.% Ag additions when tested in the 25-500 °C temperature range for sliding in air against a wide range counterpart materials, including steel, nickel-chromium based superalloy, alumina, silicon nitride, and diamond. The wear rate of such materials is difficult to quantify, because the thickness of the film changes (sometimes substantially) as the Au or Ag coalesces at the surface, and is often not reported in these studies of temperature-adaptive coating materials. All of the silver-based lubricating materials also develop lubricious double oxides at temperatures above 300 °C providing high temperature oxide adaptation mechanism discussed later in this review.

2.1.2. Control of noble metal diffusion and surface re-nucleation for high temperature lubrication

Noble-metal phase segregation and coalescence on the surface of nanocomposite surfaces is a result of the metastable condition of the coating material grown by physical vapor co-deposition of metal and ceramics

at relatively low substrate temperatures. The phenomena was first reported for the surface of YSZ-Au adaptive coatings [49], where it was found that about 10 at. % Au was sufficient to induce a rapid migration and coalescence of gold on the surface at 500 °C sliding in air. Structural analysis identified that gold was dispersed as atomic inclusions in an amorphous or nanocrystalline YSZ matrix [79]. *In situ* TEM microscopy during YSZ-Au composite annealing helped to identify the development and coalescence of Au grains starting at about 400 °C [87], which was a relatively low temperature for activation of diffusion. Even faster metal migration to the surface and coalescence was observed for a number of silver contained oxide and nitride matrix coatings, where the minimum threshold of 10-12 at. % metal additions for developing a low friction metallic tribological surface was verified [50,60-62,81].

The underlying driving forces and mechanisms of noble metal diffusion and coalescence on the surface of hard ceramic composite coatings were subjects of dedicated studies by Hu et al. [52] on an example of YSZ-Ag-Mo adaptive coatings and Mulligan et al. [88] on an example of CrN-Ag adaptive coatings. These works highlighted the importance of defects and strains in metal saturated ceramic matrices to reduce activation barriers for rapid metal migration and coalescence on the surface. The noble metal migration to the surface is achieved in the absence of the cross-thickness concentration gradients, as all coatings had uniform compositions as deposited. Figure 2 provides an example of a transmission electron microscope (TEM) study of a YSZ-Mo-Ag coating, demonstrating that initially silver is distributed as a series of disconnected nanoinclusions throughout the ceramic matrix [52,87]. These metallic silver inclusions are forced into the matrix during deposition and increase strain and interfacial energy within the composite, which reduces the activation energy for Ag diffusion [52,53]. The diffusion activation barrier is further reduced by the high vacancy concentration in the matrix. The result is a rapid migration of the metallic silver throughout the highly defective matrix structure to its surface even at moderate temperatures of <300 °C. Once at the surface, the noble metals (e.g. Ag or Au) are mobile enough to coalesce into larger clusters to further minimize their surface energy (Fig. 3). These collections of metal atoms are sufficiently large to reduce the shear strength at the interface and result in macroscopic CoF comparable to a continuous noble metal film.

The diffusion mechanism depicted in Figure 3a for delivery of solid lubricant to the hard coating surface during heating results in very rapid migration of noble metals to the surface. For example, one micron-thick YSZ-based composite coating containing 20 at. % silver as nanoinclusions will be depleted of all silver after less than 5 minutes at 500 °C [51,52]. Once the surface layer of silver lubricant is worn through, no other operative mechanism for lubrication is present within the material, therefore a means to modulate lubricant transport to the surface was desired to extend the lifetime of the solid lubricant supply within the coating material. Comparing metal diffusion of YSZ-Au and YSZ-Ag coatings, it was noted that the diffusion activation for silver starts at lower temperatures and migration rates of silver to the coating surface are also much faster, which was related to a lower melting point and higher silver mobility. To explore control over the flow of solid lubricant phases in adaptive coatings, a 300 nm thick TiN diffusion barrier patterned with an array of holes was deposited on a YSZ-Mo-Ag nanocomposite material [53]. As the silver is driven to migrate only to free surfaces, islands of silver originating from the holes were observed on the surface. Cross-sectional microscopy revealed that the silver diffused from the coating material under the diffusion barrier, out of the hole and to the top surface [53]. By tailoring the pattern in the TiN diffusion barrier, the delivery rate of the lubricant could be customized to suit the anticipated temperature range and other operating conditions. The effectiveness of the TiN diffusion

control top surface was tested in 500 °C sliding in air and shown to extend the YSZ-Mo-Ag coating lifetime by ten times without sacrificing performance in terms of a low CoF. Similar control over silver diffusion to the surface was reported for the CrN-Ag adaptive coatings with a top porous CrN cap layer [89], which thickness variation from 10 to 1000 nm was shown as an effective control over the Ag diffusion activation energy and surface mass transport at 500-600 °C. Furthermore, diffusion control layers created an opportunity for a self-guided solid lubricant delivery, which can be activated and directed by the wear process to send lubricant only where needed (e.g., the wear track) rather than to the entire coating surface. This is discussed in the next section.

2.1.3. Thermal-cycling of multilayer structures using metal-based lubrication

The patterned diffusion barriers helped to establish that noble metal lubricant would only migrate to free surfaces. This result suggested that if continuous, rather than patterned diffusion barriers are used, the wear process itself could be counted upon to activate diffusion in an adaptive nanocomposite coating. A multilayered coating with two adaptive YSZ-Ag-Mo lubricant layers and a TiN diffusion barrier between them was developed to examine this concept [54,90]. Just as a monolithic coating, the topmost adaptive coating was limited to one irreversible change. However, the top silver-depleted YSZ-Mo coating wore away after cooling to room temperature in less than 50 sliding cycles, exposing another chemically homogeneous adaptive layer buried beneath the diffusion barrier. Such exposure triggered lateral silver diffusion under the TiN diffusion barrier layer to the location in which wear was occurring, providing lubrication for thousands of sliding cycles. The process is schematically shown in Figure. 4a and an example of such adaptive coating cross-section is shown in Figure 4b. The coating cross-section was taken after heating to 500 °C for over 2 hours to demonstrate Ag diffusion to the top surface and preservation of the homogeneous composition under the TiN diffusion barrier layer.

This concept of delaying adaptive behavior in solid lubricant delivery to the wear track until needed by protecting from environmental exposure was demonstrated in a seven-layer coating with four adaptive layers separated by TiN diffusion barriers [54]. The coating endured two thermal cycles from room temperature to 500 °C and reverse, while continuously operating in a sliding friction contact and maintained CoF at 0.35-0.40 range through the temperature cycling test duration (Fig. 4c). It was noted that about one lubricant layer was consumed during each phase of thermal cycling.

2.2. Adaptive mechanisms using tribo-oxidation

The most challenging and complex adaptive mechanism in chameleon coatings is the one that pertains to tribo-oxidation, i.e. the formation of an oxide layer at contact surfaces. When the working temperature exceeds 500 °C in air, tribo-oxidation becomes a dominating process at the contact interface. Hence, the incorporation of a mechanism that self-guides the formation of a lubricious oxide becomes very desirable. The challenge remains when designing a surface that reverts back to its original 'form' during temperature cycling. A control of the tribo-oxidation process would be a necessary attribute toward a reversible adaptation.

2.2.1 Tribo-oxidation to form binary oxides

In the last two decades, various hard and ultra-hard coatings of certain transition metal nitrides have been discussed in the literature and used in industry as tribological coatings for high temperature applications [4,11]. In this class of materials, the main mechanism that leads to a reduction in CoF is tribo-oxidation. Transition metal nitrides (for example, VN, MoN, and WN) form binary oxides [28,91-93], which are lubricious at high temperatures. A crystal-chemical model by Erdemir [25] correlates low CoFs observed for these oxides at elevated temperatures with their high ionic potentials (charge/cation radius ratio), resulting in a reduction of melting points and cation screening from chemical interactions during high temperature shear. A first systematic experimental study of a large number of binary and ternary metal oxide lubricants was completed by Peterson et al. [94] for high temperature sliding Inconel X-750 alloy surfaces with applied oxide powders in considerations for aerospace bearing systems. Among other perspective oxides from this study, MoO_3 was identified to reduce CoF to about 0.2 at 700 °C tests. The lubricious nature of transition metal binary oxides can be attributed to the defect structure associated with the formation of substoichiometric compounds, commonly referred to as Magnéli phases named after Swedish scientist Arne Magnéli who first determined the structure of these compounds in molybdenum and tungsten oxides [95,96]. For example, the homologous series within the phase diagrams of these oxides have been constructed for vanadium oxides [97-100], which include the V_nO_{2n-1} series [101,102] and the V_nO_{2n+1} series [103]. For tungsten oxides, homologous phases include the W_nO_{3n-2} series and the W_nO_{3n-1} series [95,96]. Moreover, there are more than eleven different structures reported for WO_3 [104]. The structures in the homologous series consist of MO_6 octahedra that can be derived from a parent structure by crystallographic shear, leading to ordered oxygen deficiencies [95,105]. Ordered oxygen vacancies in rutile phases were investigated in details by Gardos et al. [106] for high temperature solid lubrication of aerospace mechanisms, who also suggested concepts for TiO_{2-x} Magnéli oxide structure stabilization by doping with copper [107]. The high temperature lubrication benefit of Magnéli phases is well recognized by hard coating designers [26-29,91-93,108]. For example vanadium and vanadium nitride are deliberately introduced in the traditional TiAlN tool coating compositions to reduce CoF at temperatures of 700 °C and higher with a formation of substoichimetric VO_{2-x} and a low melting point V_2O_5 as reported by Mitterer and Hovsepian et al. [26-29].

Recently, Reeswinkel et al. [109,110] used *ab initio* calculations to explore fundamental mechanisms responsible for the lubricious nature of Magnéli phases. They conducted a systematic study to correlate Magnéli oxide composition and structure with their phase formation and mechanical properties. The calculations were used to predict (i) the energy of formation per atom (a measure of phase stability); (ii) electron density distribution (a measure of bond character, strength, and extent of anisotropy); and, (iii) decohesion energy for cleavage (a measure of the energy required to separate the structure into two blocks). Moreover, their *ab initio* calculations were used to obtain the bulk modulus (a measure of a substance resistance to uniform compression), and tribologically important elastic shear constant C_{44} (a measure of the shear modulus) for various V-, Ti-, Mo-, Re- and W-based oxides (Fig. 5a). Reeswinkel et al. [109,110] established that Magnéli phases displaying distorted metal-oxygen octahedral architecture, for example WO_3, result in large inter-layer distances and hence lower C_{44} values as compared to the phases with undistorted octahedral coordination, such as ReO_3. They also showed that the decohesion energy in Magnéli oxides is governed by a shielded Coulomb interaction between the inter-layers in their structure. Such inter-layer distance dependence results in weaker coupling as the layer distance is increased, which causes the formation of easily plastically deformable structures. Hence, solid lubricants can be designed based on control of the distance between layers by changing oxide composition or

structure. Out of the modeled structures, the V_2O_5 system had shown the largest separation distance between metal-oxygen bonding localized in (002) planes (Fig. 5b). This result is consistent with a number of experimental observations for high temperature lubrication with vanadium contained hard coatings reviewed by Franz and Mitterer [29] most recently.

2.2.2 Tribo-oxidation to form ternary oxides

A concept of tribo-oxidation to form ternary oxides was found to be a promising alternative to the Magnéli phase lubrication at the sliding contact of hard coatings [34]. There are several successful adaptive coatings made of transition metal nitrides and soft metals that can form lubricious ternary oxides at the surface contact. In fact, the first reported temperature adaptive PbO-MoS_2 composite coating by Zabinski et al. [44] relied on the $PbMoO_4$ ternary oxide to extend lubrication to 1000 °C. In a detailed study on lead molybdate tribology, this ternary oxide was found to provide a long endurance and CoF within 0.3-0.4 at 700 °C in air with sliding against nickel-chromium based superalloy but abrasive at low temperatures [47]. In follow-up developments of the high temperature adaptive solid lubricants with ZnO-MoS_2 and ZnO-WS_2 compositions, both $ZnMoO_4$ and $ZnWO_4$ were identified at sliding contacts and linked to a reduced CoF at elevated temperatures [111,112]. Prasad et al. [113] had reported in details on the ZnO-WS_2 mixed powder burnished coating, where zinc tungstate formation provided about 0.2 CoF and long endurance in sliding against a steel counterpart at 500 °C in air.

In most recently developed adaptive hard coating compositions, Ag is a widely accepted metal to facilitate ternary oxide formations in high temperature sliding. Silver has several desirable properties: (1) it is a soft metal with an easy shear which can effectively lubricate at moderate temperatures (300-500 °C) as discussed in the earlier section of this review; (2) Ag-O bonds are relatively weak, as compared to transition metal oxides, and when incorporated in a ternary oxide crystal structure enhance shearing of crystal planes and lowering melting point of the original binary metal oxide; (3) elemental Ag does not oxidize readily and would significantly enhance tribological properties of the surrounding oxide phases by providing ductility and enhancing toughness; and (4) Ag is environmentally benign for coating manufacturing. Some examples of adaptive materials with silver additions to form lubricious ternary oxides at higher temperatures include Mo_2N-Ag [57-59,85,114], MoCN-Ag [86], VN-Ag [60], NbN-Ag [61], and TaN-Ag [62]. These composites form silver molybdates, vanadates, niobates, and tantalates, respectively, in the sliding contact area.

An important focus of recent studies of ternary oxides formed by tribo-oxidation process when using adaptive coating compositions is to understand the mechanism that leads to their lubricity. Detailed investigations of silver molybdate ternary oxides helped considerably advance understanding frictional adaptation mechanisms in such solids [51,114,115]. Silver molybdates with a broad operation temperature were created by producing Mo_2N-MoS_2-Ag adaptive coatings [57-59]. The addition of sulfur was found to be a necessary catalyst that facilitated the formation of the lubricious ternary oxides [56]. Three low friction silver molybdate phases were explored [58]: (1) Ag_2MoO_4 cubic system of Fd3m space-group structure; (2) $Ag_2Mo_2O_7$ and (3) $Ag_6Mo_{10}O_{33}$ with P1 space groups of triclinic symmetry. The measured CoF for these phases was found to be in the 0.1-0.2 range when tested against silicon nitride at temperatures in the vicinity of 600 °C. All three phases were found to have melting points slightly above 500 °C. For example, the structure of the Ag_2MoO_4 system consists of a mixture of Ag_2O and MoO_3 arranged in a spinel structure, which may be viewed as a layered structure with mixed AgO and MoO_3

layers separated by a silver layer as shown in Fig. 6(a) [58]. During sliding at high temperatures, the weaker Ag–O bond (220 kJ/mol compared to 560 kJ/mol for the Mo-O bond) may shear easily and partially break, which leads to both low friction and appearance of smooth plate-like morphology in the surface of the wear track (Fig. 6b). Raman spectroscopy analysis performed on these morphological features had confirmed the silver molybdate oxide presence. The structure of $Ag_2Mo_2O_7$, however, consists of $[Mo_4O_{16}]^{8-}$ chains linked through O–Ag–O bridging bonds to form a 3-dimensional network [58]. This relatively weak bridging bond accounts for the low CoF observed for this system as well. Another feature of this system was negligible wear, as the formation of the ternary oxides on the surface of the wear track results in the material build-up. In the result, the wear could not be measured even after long duration tests at 600 °C with 300,000 sliding cycles. This interesting phenomena is yet to be explored for wear track self-healing effect by the oxide growth triggered with tribo-oxidation reactions.

The adaptation mechanism with silver vanadate formation when using VN-Ag [60] nanocomposite coatings was also investigated in the literature. This adaptive coating was found to form two silver vanadate phases on the surface, namely $AgVO_3$ and Ag_3VO_4, in addition to vanadium oxide. The addition of sulfur was not required to form these structures. The thermal stability of the Ag_3VO_4 lubricious phase was investigated using *in situ* Raman spectroscopy and temperature-dependent X-ray diffraction. It was found to behave as a metastable phase, which segregated into silver and a liquid phase ($Ag_3VO_4 \leftrightarrow Ag$ + liquid) when heated to 450 °C. The phase segregation and melting were identified to be the main mechanisms that reduce the CoF of the VN-Ag composites to 0.10-0.25 in sliding against silicon nitride balls at above 500 °C in air [60].

Most recently, Stone et al. [61,62] investigated other ternary oxides with higher melting temperatures, namely silver niobate [61] formed within adaptive NbN-Ag coatings and silver tantalate [62] formed with adaptive TaN-Ag coatings. A comprehensive study of silver tantalate was carried out since it displayed outstanding tribological properties at elevated temperatures. Silver tantalate was created either in powder form using solid-state synthesis or by reactive magnetron sputtering using silver and tantalum sputtering sources to form $AgTaO_3$ (in O_2 environment) or TaN-Ag (in N_2 environment). The presence of nanoparticles of segregated Ag in the coatings was found and increased coating toughness [62]. Analysis of the chemical and structural composition in the wear track after tribotesting at 750 °C revealed multiple individual ($AgTaO_3$, Ag, Ta_2O_5) and mixed ($AgTaO_3$/Ta_2O_5) phases at the sliding interface. All of these were linked to the reduced CoF. However, the main contribution was thought to come from the $AgTaO_3$ phase. To better understand the mechanisms of friction reduction with $AgTaO_3$ at elevated temperatures, a bright field TEM (BFTEM) was used to analyze the structural and the tribochemical changes that occur in the sub-surface region of the wear track on a $AgTaO_3$ coating surface (Fig. 7). BFTEM images taken after 10,000 sliding cycles (about 600 m of the total sliding distance) revealed that the surface region consists of Ag clusters surrounded by Ta_2O_5 while further away from the sliding interface the $AgTaO_3$ remains intact [62]. Unlike the case of silver molybdates and silver vanadates, the Ag-O bond in the $AgTaO_3$ structure is stronger and requires both high shearing strain and temperature to break. One potential challenge to overcome with $AgTaO_3$ coatings is a dependence of their behavior on the contact load, which was found recently to provide a rise of CoF from 0.04 to 0.15 when the load on a 6 mm diameter Si_3N_4 ball was increased from 1 to 10 N at 750 °C tests in air [116]. Performed molecular dynamic simulations helped to explain such load dependent behavior by silver extrusion from the contact zone under an increased contact pressure, which leads to a higher shear strength and increased porosity of the contact surface.

There are fewer articles that are published on the high temperature tribological properties of coatings that include copper as a soft metal capable of double oxide phase formation instead of silver. Gulbinski et al. investigated copper vanadates [117] and copper molybdates [114] for high temperature lubrication. They reported that copper vanadates are even much less thermally stable than silver vanadates. The CoF of these materials in sliding against alumina balls was found to decrease to around 0.3 with an increase in temperature down at 600 °C. The CoF of the copper-based materials was, however, found to be higher than the CoF of their silver-based counterparts. A more detailed investigation of tribo-chemical mechanisms that occur at the surface of these copper based materials may need to be performed. For example, a study by Ozturk et. al [118] for a room temperature behavior of TiN-Cu, CrN-Cu, and MoN-Cu composite coatings demonstrated that only in the case of MoN-Cu coating there was a friction reduction linked to the formation of copper molybdate oxides. In addition, CrN-Cu friction behavior was improved when the temperature was increased from room to 150 °C due to a complex oxide formations on the surface [119].

Another promising approach with ternary metal oxides is to use these in a synergistic tribochemical interaction of the coating and counterpart materials to form a lubricous surface oxide. Examples provide Cs_2WOS_3 studied by Rosado et al. [120] and Cs_2MoOS_3 studied by Strong and Zabinski [121] for adaptive high temperature lubrication in rolling and sliding against Si_3N_4 ceramic counterparts at 600-800 °C range in air. In these coating compositions, cesium was found to be critical to modify silicate tribofilm, which is formed as a result of a high temperature tribo-oxidation of Si_3N_4 ball counterparts. Cesium, as well as sodium, calcium, lithium, and potassium are some of the known glass network modifiers, which provide monovalent ions disrupting glass bonding. Their additions to the coating composition can be used to create low melting point silicate glass for an effective lubrication at elevated temperatures. For example, the friction coefficients of cesium oxythiomolybdate coatings against Si_3N_4 balls were reported as low as 0.03 at 600 °C [121]. The Cs_2MoOS_3 coatings of about 1 μm thickness could maintain a low CoF for over a million sliding cycles at high temperature sliding regimes due to the formation of a low melting point cesium silicate tribofilm. At the moderate temperatures, the coatings had a CoF in the range of 0.2 attributed to an oxide softening, and at room temperature the CoF was higher due to an abrasive wear. This approach, where the counterpart material steers contact tribo-chemistry reactions to form high temperature lubricant is a promising direction to engineer self-adaptive surfaces, which not yet broadly explored with temperature adaptive hard coating compositions.

2.3. Adaptive mechanisms using structural transitions

Both temperature cycling and repeated straining of surfaces in sliding and rolling contacts can be used for structural surface evolutions. One well-documented example is the reorientation of initially randomly-oriented polycrystalline hexagonal lubricant solids (MoS_2, WS_2, WSe_2, graphite, etc.) or their amorphous → crystalline surface transformations to provide contact surfaces with hexagonal basal planes oriented parallel to the surface [122-131]. This leads to a considerable reduction of both friction and wear, as such easy to shear planes provide low friction surfaces that are also inert to oxidation. The reorientation is observed even under ambient temperature conditions. Hu et al. [128] had used an *in situ* microtribometer compatible with a focused ion beam (FIB) for contact interface TEM sample preparation to study friction induced structure transitions in Mo-W-S-Se nanocomposite coatings, where CoF was recorded about 0.02

against SiC at room temperature in humid air. The experiments demonstrated that few monolayer thick and highly (002) oriented hexagonal layers are quickly formed at the contact surface from an initially poorly crystalized and randomly oriented material (Fig. 8) [128]. Recently, an ultra-low friction was reported by Gustavsson et al. [132] for fully amorphous W-S-C coatings, where friction induced surface structure transition provided a few monolayer thick hexagonal WS_2 tribofilm that resulted in CoF values below 0.01 for sliding in humid air against steel balls. Once such ultra-low friction hexagonal surface layers are formed the wear rate decreases dramatically. For example, wear rates of 2 x 10^{-8} $mm^3N^{-1}m^{-1}$ were reported by Hamilton et al. [129] for some of the MoS_2 based adaptive chameleon coating compositions tested under temperature variations from -80 to 180 °C. In this work, it was noted that for such ultra-low wear rate coatings, their sliding behavior was strongly affected by the temperature and linked to almost frictionless (CoF of 0.02-0.04 in self-mated sliding contacts) relative slip of hexagonal basal planes at temperatures above -50 °C.

Similar mechanisms were also observed with initially amorphous carbon solids, where the materials experienced hexagonal structure crystallization in the tribological contacts with the basal planes parallel to the sliding contact. One such example would be the development of a graphitic transfer layer on the surface of initially amorphous highly tetragonal bonded diamond like carbon (DLC) coatings, which involves sp^3 to sp^2 interatomic bond configuration changes [124-126]. While the exact mechanisms of such structure transitions is still being debated – frictional heat-actuated short circuit diffusion [128,130] or mechanically actuated shifts of atom clusters [131] - the net result allows release, crystallization, and re-orientation of basal planes favorably from stored amorphous or poorly solid lubricant reservoirs.

Since hexagonal lubricant solids are normally very soft, their incorporation in hard composite coatings was one of the widely explored approaches in the literature. For example, the ability of amorphous carbon to undergo structural transformation and form a lubricious graphitic-like film was explored in a number of hard coatings with TiC-DLC, WC-DLC, CrC-DLC compositions when using both hydrogenated and hydrogen-free DLC phases [72,133-147]. In these composites, amorphous sp^3 bonded carbon formed a thin, “tissue” layer around few-nanometer sized transition metal carbide grains, providing a unique combination of high hardness and reduced friction. TiC-DLC composites produced by sputtering were reported to have Vickers hardness in excess of 4000 HV0.05 and maintain CoF at about 0.08-0.14 against a steel counterpart at room temperatures [141]. The benefits of amorphous carbon boundary phase separating nanocrystalline TiAlNC and TiC grains for coating hardness and tribological performance optimization were discussed in detail by Stueber et al. [148-150] and Zehnder and Patscheider et al. [142,143]. More recently, Gassner et al. [146] studied thermal stability of the hydrogenated amorphous carbon tissue (a-C:H) in CrC-a-C:H composites for 200-400 °C sliding operations. It is also important to note that carbide-DLC composite coatings have excellent resistance to both impact [151], scratch [72], and indentation [70] surface loading. The amorphous carbon tissue deflects cracks and allows a large degree of coating deformations, resisting fracture and delamination, even as DLC based nano-composite coating hardness is typically measured within 20-30 GPa range. Such unique mechanical performance helps to achieve a load-adaptive tribological coating concept, where high hardness surface can absorb deformation energy without brittle fracture [69,72,137].

A drawback of composite coatings with DLC phases is temperature limitations, where sp^3-sp^2 bond transformation, oxidation, and formation of volatile products starts at about 300-400 °C range for both

hydrogenated and hydrogen free DLC variants, the latter are being more temperature stable in non-oxidative environments [146,152-155]. Because of such temperature sensitivity of amorphous carbon in air, even for composites with intrinsically temperature stable and oxidation resistant matrix, e.g. TiB_2-DLC coatings, the useful temperature regime is limited to below 300 °C [156,157]. This can be mitigated to some degree by thermal oxidation stabilization of DLC network with additions of metals [158-163] and nitrogen [164-167]. For example, 5-20 at.% silicon additions were reported to improve DLC network stability up to 400-500 °C in air [158,160,163].

Similar to DLC in nanocomposite hard coatings, multiple attempts were carried out to develop coatings that incorporate transition metal dichalcogenide (TMD) solid phases. These approaches normally yield lower friction and better temperature stability as compared to carbon phase lubricated composites, but they also provide lower composite coating hardness values and abrasive wear resistance. Bae et al. [168] were first to report TiN-MoS_2 composite coatings made of 50 nm sized TiN nano-crystalline matrix with dispersed poor or nano-crystalline MoS_2 phase and test these at elevated temperatures for sliding against Si_3N_4 counterparts in air. They found that up to about 300 °C, the CoF was of the order of 0.1 and increased to about 0.7 as the test temperature was raised to 400 °C. This was was linked to the abrasive nature of the newly formed MoO_3. Interestingly, they also reported a drop in CoF to 0.3 for tests at 700 °C, which at that time was not linked with the Magnéli phase lubrication. Gilmore at al. [156,169,170] reported more recently on the structure and properties of both TiN-MoS_2 and TiB_2-MoS_2 composite coatings, where a hardness of 20 to 30 GPa could be achieved, depending on the growth route. In their TiB_2-MoS_2 study, it was shown that CoF below 0.1 against steel counterpart can be maintained up to 400 °C, which is a substantial improvement as compared to the TiB_2-DLC coating temperature stability [156].

Combinations of TMD and DLC phases, such as in WC-WS_2-DLC nanocomposite coatings [68], was also found to be beneficial for adaptive tribological behavior, where low CoF and wear rates were achieved for both dry and humid environments. Similar results were obtained with WC-MoS_2 composites, where CoF against steel ball is about 0.07-0.15 in air (depending on humidity) and 0.02-0.04 in vacuum [171,172]. In studies by Polcar and Cavaleiro et al. [32,173-175] a number of amorphous TMD compositions alloyed with carbon and nitrogen was explored to improve TMD oxidation and temperature stability as well as to maintain hardness of about 10 GPa for abrasion wear resistance. For example, both Mo-Se-C [174] and W-Se-C [175] amorphous coatings were suggested as alternatives to W-S-C compositions for improved oxidation stability and endurance in humid air. Fominsky and Grigoriev et al. [176,177] recently reported W-Se-C and Mo-Se-Ni-C composite coating, where improved hardness and elastic deformation was associated with a complex carbide-TMD-metal composite structure. Composites coatings made of W_3O-WSe_2 were also found to improve oxidation resistance for sliding contacts in humid environments [178]. Unfortunately, most of the published tribological studies with TMD based composite coatings only provides results from room temperature sliding tests. Nevertheless, the W-S-N ultra-low friction coatings in already mentioned studies by Polcar and Cavaleiro were demonstrated to have good temperature stability up to 400 °C in air in tests against steel counterparts and maintained CoF values below 0.01 in the 100-300 °C temperature range [173].

From the above discussions with carbon and TMD based adaptive lubrication in hard composite coatings, the embedded amorphous or poorly crystallized lubricant reservoirs are vulnerable to oxidation and need be protected in higher temperature environments until they are ready to be used for contact surface

structural transition. One approach for this is to seal lubricant reservoirs inside oxide ceramic matrices as small inclusions. The small size of such inclusions is required to keep the relative hardness value of such composite material higher. For example encapsulation of 2-3 nm size MoS_2 inclusions in amorphous Al_2O_3 was used to prevent MoS_2 oxidation at ambient conditions and allow for low friction coefficients and extended coating wear endurance in vacuum [70]. There were also several reports with detailed microstructure characterizations where inclusions of both MoS_2 (for dry or space environment) and DLC (for humid or ambient environment) were encapsulated in YSZ and Al_2O_3 matrices to be protected against oxidation at above 500 °C exposure to air [55,179,180]. *In situ* Raman spectroscopy and post-test cross-sectional TEM confirmed hexagonal MoS_2 solids in the contact zone, when the temperature is cycled from high to low.

One interesting and relatively less explored concept is MoS_2 encapsulation by $MoTe_2$ hexagonal layers in a closed-shell structure (Fig. 9a) [181]. The shell was comprised of few monolayer thick $MoTe_2$ layers providing an effective oxidation barrier during high temperature exposure and also led to formation of a tellurium molybdate oxide on the wear track surface, protecting underlying MoS_2 inclusions from oxidation [130]. Figure 9b provides an example of CoF variation of a core-shell MoS_2-$MoTe_2$ nanocomposite coating for sliding against a Si_3N_4 ball at 450 °C in air. This figure insert shows a Raman spectra from the wear track surface, from which formation of hexagonal MoS_2 and complex MoO_3 and $[TeMo_6O_{24}]_6$- oxides on the surface is evidenced [130]. Such core-shell concept for the solid lubricant protection helps to maintain a low CoF over a broad range of temperatures in air and provide complex composition oxides which can provide lubricity at high temperatures.

The temperature induced structural evolutions can be used for another important high temperature wear resistant coating characteristic – prevention of coating softening. The experience with hard coatings for tool surface protection indicates the benefits of structural evolution in immiscible and metastable material systems which can undergo phase reconstructions, resulting in improved material hardness. For example, Mitterer et al. introduced TiN-TiB_2 hard nanocomposite coatings with high temperature stability which could maintain 40-50 GPa hardness up to 1000 °C [11,20,182]. When exploring structural evolutions in this system, Mayrhofer et al. [183,184] identified temperature activated hardening in supersaturated cubic TiBN with the formation of hexagonal TiB_2 precipitates separated from cubic TiN grains by a thin amorphous boron enriched layer. There are also detailed studies of the hardness increase in spinodal decomposition in supersaturated TiAlN coatings with the formation of coherent fcc AlN domains for strain field modulations [185,186]. These self-hardening materials are good examples from hard tool coating development approaches, which demonstrate that it is possible not only to preserve, but actually increase coating hardness by 10-20% at temperatures exceeding 500 °C. A discussion of temperature activated structural evolutions in hard coatings and design approaches for age hardening can be found in a comprehensive review by Mayrhofer et al. [12]. As an additional benefit, segregation of amorphous BN from supersaturated TiBN can potentially lead to high temperature self-lubrication with an amorphous to h-BN surface layer transformation. A formation of BN phase in over stoichiometric TiBN coating compositions was reported to decrease friction, but the wear resistance also decreased [187]. While the lubrication mechanism can be a subject of further studies and optimizations, tests of hard TiBN coatings on tool dies by Paschke et al. [24] showed a reduction of adhesion between working piece and the tool surface for 800 and 1150 °C forging operations. The incorporation of solid lubricant constituents within

age-hardened microstructures is one potential opportunity for future developments of hard coatings with temperature adaptive mechanisms.

2.4. Broad temperature range adaptation

Each of the mechanisms described above provides effective lubrication within a relatively narrow range of temperature conditions. For applications over a broader range of temperatures, e.g. spanning from room to about 1000 °C, a material employing multiple adaptive mechanisms may be needed. The term 'chameleon' coating was coined for the hard coatings with embedded solid lubricant reservoirs to *reversibly* change surface chemistry and composition upon the change of the environment [69,71,72]. The concept of such reversible adaptive surface behavior (Fig. 1) was first demonstrated with WC-DLC-WS_2 coatings for air to space environment cycling [68,188], and later extended to include higher temperature adaption with more complex YSZ-Au-DLC-MoS_2 [55] and Al_2O_3-Au-DLC-MoS_2 [179,180] coating compositions. The DLC phase in these chameleon compositions increased coating hardness and provided a source of carbon for surface graphitization following carbon sp^2-sp^3 electron hybridization change and structural transformation in the wear surface for humid environment lubrication. This conceptual design works fairly well to maintain CoF within 0.02-0.2 range for temperatures up to 500 °C [179]. It is, however, challenging to prevent DLC degradation (both through structure relaxation to graphite and oxidation) at higher temperatures. Other ways to 'store' during high temperatures exposure and 'deliver' carbon to the surface at lower temperature cycling were also pursued. For example, in a recent work by Shtansky et al. [86] graphitic layer formation in wear tracks of MoCN-Ag coatings was shown and associated with a reduced CoF to about 0.4 in sliding against Al_2O_3 counterparts below 100 °C. The composition had higher friction in the 100 to 400 °C range before the onset of lubrication with metal oxides in the 400 to 700 °C range.

Crossing over mid-temperature ranges from the conditions when transition metal dichalcogenides and carbon are the best solid lubricants to the conditions for shearing Magnéli and double metal oxides at above 600 °C is a primary challenge, which was facing high temperature adaptive coating developers from the early works with PbO-MoS_2 and ZnO-WS_2 adaptive coatings [44,111]. One approach is to combine diffusion-based lubrication at above 300 °C and transition metal oxide lubrication at above 600 °C. For example, YSZ-Ag-Mo coatings were explored with the idea that silver would provide lubricity in the mid-temperature range and molybdenum oxides at the high temperature [50,51,63]. Given the behavior of silver, which was observed to form a continuous surface layer as discussed in the metal lubrication section, the underlying YSZ-Mo was protected from the ambient environment, inhibiting oxidation of the Mo. Once the temperature is increased, the softened Ag is extruded from the wear track, exposing Mo at the surface to the ambient air resulting in its oxidation. While abrasive at lower temperatures, the newly formed MoO_3 provides a low shear interface at temperatures >600 °C. This material design provided broad temperature lubrication by incorporating different elements that work together to facilitate their independent lubrication mechanisms. One drawback of these materials is short lifetimes for temperatures between 400-600 °C, a region in which noble metal lubrication and simple metal oxide lubrication are marginal.

Hard coating compositions that operate by combining metallic silver for lubrication below 300 °C, form easy to shear ternary oxides at 300-600 °C, and Magnéli oxides for lubrication above 600 °C is a

breakthrough approach to cross over the mid temperature range and achieve stable friction behavior from room to 800 °C in air. However, the formation of ternary oxides, such as silver molybdate, provides some challenge. In post-test analysis of the YSZ-Mo-Ag composites the contact surfaces were found to be composed primarily of Ag from 25 °C to 500 °C and of MoO_3 at temperatures above 500 °C. This lack of reactivity between Mo and Ag may have been due in part to the lack of contact between the elements due to rapid diffusion of silver to the coating surface [50,51]. To promote silver molybdate compound formation and to decrease the CoF at temperatures below 300 °C, small fractions (less than 10 at. %) of MoS_2 were added to YSZ-Mo-Ag coatings [56]. Such introduction of sulfur via MoS_2 additions enhances Ag-Mo reactivity in two ways: (1) provision of additional chemical reaction pathways, e.g. the Ag-S-Mo system results in the reaction $MoS_x+Ag \rightarrow AgMoS_x$, followed by an energetically favorable replacement of sulfur by oxygen at elevated temperatures [189,190]; and (2) reduction of the silver diffusion rate by creating a more chemically reactive environment (Ag-S) within the material. The latter slows silver segregation to the coating surface prior to reaching the reaction temperature for Ag-Mo-O compound formation. Silver was shown in micron-scale YSZ-Ag-Mo composites to diffuse to the surface in minutes, completely depleting the silver content from the YSZ-Mo matrix, even at temperatures as low as 300 ^{o}C [52,53]. Subsequent findings indicated that MoS_2 reduced Ag diffusion rates, which may increase the time for which Ag and Mo are in contact with one another, promoting formation of double metal oxides at temperatures >300 ^{o}C [58].

On the basis of these two mechanisms of sulfur involvement in silver molybdate formation and silver diffusion, this MoS_2 addition therefore has the effect of a low temperature lubricant, an endurance extender for the lubrication with metallic silver, and a catalyst for the ternary oxide formation. The friction coefficient dropped to below 0.2 for sliding against silicon nitride counterparts and was stable from room to 700 °C for a series of YSZ-Mo-Ag-MoS_2 coatings with different compositions, where hexagonal MoS_2 and silver molybdate formation were observed via Raman spectroscopy and X-ray diffraction (Figure 10) [56]. Additional work was focused on the challenging middle temperature zone (300-500 ^{o}C) by Stone et al. [59], where formation and structure evolutions of intrinsically layered silver molybdate and silver tungstate phases was analyzed with both experimental and molecular dynamic simulation studies to explore the origin of CoF below 0.2 in tests against silicon nitride balls. The results of these studies are consistent with earlier reports by Gulbinski et al. [114,115] that silver molybdate monolithic films can provide CoF in the 0.2 range against alumina balls at 400-500 ^{o}C. The addition of sulfur in Mo_2N-Ag-MoS_2 composite coatings promotes such phase formations to start from about 350 ^{o}C [58], which also results in a lower CoF when compared to Mo_2N-Ag coatings tested at 400 ^{o}C [85].

Wear rates of these broad temperature range adaptive coatings were moderately low, and the friction coefficients were the lowest reported for any material over this temperature range. This demonstrated an additional level of synergistic interactions of elements and phases within a tough, inert matrix as a way forward for broad temperature lubrication. Recent works were focused on producing adaptive nanocomposite coating materials via magnetron sputtering rather than a complex hybrid pulsed laser deposition-sputtering processes used for the earlier YSZ based adaptive coatings. Synthesis of broad temperature adaptive hard coatings on a larger scale offered with magnetron sputtering was investigated for Mo_2N hard matrix coatings with nanoscopic MoS_2 and Ag lubricant phase inclusions [34,57,58]. In addition, a number of bulk hard composites incorporating multiple lubricant phases and demonstrating similar mechanisms were also reported [35].

3. Future opportunities and challenges for high temperature solid lubrication

The previous section reviewed mechanisms which are either currently used for high temperature adaptive hard coatings or have been studied in the great detail and are emerging in practice. Their practical use will verify the benefit of materials demonstrating multiple synergistic adaptive mechanisms for lubrication over a broad range of temperatures. In this section of the review, we will attempt to highlight some alternative approaches, which are in their early development stage and can provide additional capabilities for future hard coatings with adaptive high temperature performance.

3.1. Easy to shear and high temperature stable coatings within MAX phase family

One example of a chemically stable and lubricious material class may be found within the family of MAX phases [35,191]. These phases have an intrinsically layered covalent/metallic bonded structure, where transition group metals (M atoms) form closed packed layers, which are interlayered with A-group elements (A atoms), while C or N atoms (X atoms) are occupying some of the octahedral interstitials in closed packed M atom layers [192,193]. Such a layered solid was expected to shear easily along metal basal planes, which had given rise to machinable bulk ceramics made of Ti_3SiC_2 and Ti_2AlC reported by Barsoum et al. [191,194-196]. Studies with a single crystal Ti_3SiC_2 shear under lateral forces on a microscopic scale, had indeed demonstrated CoF as low as 0.002 (detection limit of the used instrument with probes micro-fabricated from doped silicon) along the base planes [197,198]. However, macroscopic size polycrystalline MAX phase materials normally yield friction coefficients anywhere between 0.4 and 1.0 in sliding against nickel-chromium based superalloys and alumina counterparts, and were the subject of detailed tribological investigations by Gupta et al. [35,64-66]. In a review of the MAX phase tribological studies by Gupta and Barsoum [35], the authors identified several types of transfer films formed in the contact depending on the composition of the MAX phase, the counterpart material, ambient environment and temperature. Developing the idea of chameleon high temperature contacts, they added Ag to the MAX phase compositions [64,199]. This resulted in a double-layer tribofilm chemistry with a top layer consisting of a fine mixture of metal oxides, and the thicker underlayer made of a mixture of carbides, MAX phases and silver intermetallics (Fig. 11a). Such a double layer tribofilm resisted abrasive wear and provided adaptive tribo-oxide surface reactions for lubrication in thermocycling over the 25-550 °C temperature range [199]. Figure 11b shows an example of CoF variation during temperature cycling when sliding a Ta_2AlC-Ag composite against a superalloy surface [35]. Ta_2AlC-Ag and Cr_2AlC-Ag composites had friction coefficients of 0.3-0.4 and demonstrated low wear in 550 °C in airfoil bearings with the Inconel 718 superalloy as a counterpart [64].

The full potential of MAX phases in terms of easy shear and chemical stability at relatively high temperatures is yet to be realized for solid lubrication, provided that the following challenges can be addressed: i) identification of temperature stable MAX phases (and similar metallic-covalent layered solids) which have a very low shear strength between intrinsically layered basal planes; ii) cost effective technologies for preparing surfaces with MAX phase basal planes aligned along the sliding contacts. The recent development of computational tools has allowed researchers to design and evaluate MAX phase solids from a perspective of stable structures and bonding configurations, as well as predict their mechanical properties, including shear modulus and strength along specific crystallographic directions.

Music and Schneider with co-workers [200-202] systematically applied *ab initio* calculations to correlate valence electron concentration with structure, density of states, and mechanical properties in MAX phases and similar nano-laminated solids. For example, using crystal-orbital Hamilton population theory to investigate bonding strengths along specific crystallographic directions, they have shown that the easiest shear occurs between weaker non-directional M–M and M–A bonds in M_2AlC carbides [201,203].

While applying *ab initio* computational approaches, Sun et al. [204,205] classified M_2AlC systems into two large groups depending on the valence electron density distributions: weakly coupled (for M=Ti, Zr, Hf) and strongly coupled (for M=V, Nb, Ta, Cr, Mo, W) nanolaminates. Extending these approaches further to explore shear in temperature stable MAX phase solids, they showed that the use of Y, La, and Sc for M layers will reduce basal plane shear modulus by a factor of 3-4 as compared to Ta_2AlC and Cr_2Al. The comparison of these two groups predicted mechanical properties shown in Figure 12a [206]. The predicted shear modulus reduction should also lead to a considerable reduction of CoF along the basal planes, which remains to be experimentally verified. Music at al. [207] also have shown that once the basal slip occurs and the M-A interlayer bonds are broken, the shear stress required for subsequent basal plane sliding can be additionally reduced by about of a factor of two. Figure 12b demonstrates this principle on an example of a basal slip in a relatively stronger and thermally stable Nb_2AlC [207]. It predicts that the Nb-Al bond breaks at about 30% strain, while the Nb-C bond remains intact. The abrupt shear stress reduction after the basal plane slip onset is maintained on the lower level for the rest of the straining. Using similar theoretical approaches based on the electronic density of state calculations, it was recently shown that ductile ceramic materials with intrinsically layered structures are possible with the metal-boron-carbon chemistry, e.g. Mo_2BC, Ta_2BC, W_2BC [202,208]. These can potentially have higher thermal stability and also contain boron, which can help to form lubricous boron oxides and boric acid lubricants at low temperatures in ambient environments [209].

For a low friction behavior based on the above theoretically predicted easy shear processes, the MAX phase structure orientation with basal planes parallel to the surface is expected. Advancements in thin film technologies may offer such opportunities, where ion bombardment and deposition flux densities can be utilized for the growth of highly textured films. A review by Eklund et al. [210] for MAX phase thin film growth, indicates that such highly textured film synthesis is possible but many hurdles exist, including prevention of phase separation, control of the texture evolution, keeping the desired stoichiometry across film thickness, etc. From this comprehensive review, the best results were obtained in materials sputtered from elemental targets at higher substrate temperatures, although there are also reports with reactive sputtering, cathodic vacuum arc, pulsed laser deposition, and chemical vapor deposition approaches. Another challenge is achieving a thermally stable, easy shearing interface contact without formation of abrasive particulates. Investigations of (0001) textured Ti_3SiC_2 produced by elemental target sputtering on an epitaxial matched sapphire (0001) surface, showed that film tends not only to shear but also delaminate between basal planes and produce kink sites, forming abrasive debris at moderate contact loads [211]. The majority of thin films deposited from MAX phase targets yield multiphase compositions where crystalline and amorphous carbide phases are also present. Tribological studies of such composite films show CoF at the 0.3-0.4 range for sliding against steel, WC and Al_2O_3 counterparts [212-214], and there are reports that increased temperatures up to 500 °C decrease friction coefficients in association with a TiO_2 formation [215]. We also note that a very low friction coefficient of 0.1 in ambient condition was observed with the above-mentioned epitaxial grown single phase Ti_3SiC_2 films in tests against alumina balls with very small contact pressures, when the sliding was governed by shearing of the TiO_2 on the

surface and not of the MAX phase basal plane shear [211]. Thus, the route of the intrinsically laminated metallic/covalent bonded solids, such as MAX phases and materials with similar structures, is attractive but yet challenging and remains to be explored further for high temperature adaptive lubrication.

3.2. Compliant and load adaptive surfaces with vertical nanotube arrays

Novel temperature and load adaptive coatings may be created using arrays of vertically aligned nanotubes as a load bearing and compliant material, which is subsequently filled with solid lubricants. For example, such structures were produced by infiltrating MoS_2 electrochemically in vertically aligned carbon nanotube (CNT) coatings grown on Inconel alloy substrates [63]. These adaptive structures provided much better wear resistance under the same operating conditions than MoS_2 coatings without compromising friction coefficient values. The CNT-MoS_2 composite coatings displayed environmental adaptation by maintaining CoF values of 0.04 and 0.09 in sliding against alumina balls when cycled between dry and humid air. Adaptation with temperature from room to 500 °C was also demonstrated by infiltrating lubricious silver molybdate powders into carbon nanotube coatings [216]. The excellent performance of these composites was shown to be a result of: (1) the high strength and fracture toughness provided by the nanotubes; (2) the self-lubricating nature of the CNTs as they unzip into graphitic phases when worn, which is confirmed with a study of multiwall CNT arrays under sliding contacts [217]; (3) the lateral-support provided by the solid lubricants to the CNTs preventing them from breaking under relatively high loads [63].

Boron nitride nanotubes (BNNTs) would potentially be another alternative as a compliant and load adaptive lubricating material. BNNTs are anticipated to demonstrate similar or better performance than CNTs in tribological applications, as they are intrinsically more oxidation resistant. Recent studies of individual BN nanotubes under an AFM scale contact support this observation [218]. Investigations by Golberg et al. [219] also revealed that, unlike CNTs, BNNTs had the effect of accumulating a bending curvature rather than uniformly curl and kink under a compression load. Moreover, hexagonal boron nitride is a widely used lubricious material that has the added benefit of being thermally stable at temperatures of up to 1000 °C. For example it is used as a lubricating additive in bulk ceramic composites, e.g. Si_3N_4 matrix based, for high temperature tribological part manufacturing [220]. Unzipping of BNNT in the sliding contact under a combination of temperature and tribo-chemical processes and material re-orientation to provide h-BN lubricious surface is an adaptive possibility, which yet remains to be investigated. A nanotube based self-lubricating composite may, therefore, be designed as a highly compliant surface to incorporate load adaptive behavior and enable solid lubrication in various environments and in a broad temperature range.

3.3. Low friction and chemically inert 2D surfaces

The class of 2D materials is rapidly expanding due to their intriguing physical properties enhanced with multiple heterostructure possibilities reviewed recently by Geim and Grigorieva [221]. From the solid lubrication perspective, 2D materials of few monolayer thickness and weak Van der Waals interlayer bonding provide ideal low shear and inert surfaces. When these are combined with mechanically rigid substrates for contact load support, an effective contact lubrication is logically expected. Several reports had followed on friction reduction with 2D materials, including graphene and few monolayer hexagonal BN, when tested at

nano- and micro- contact loading conditions [69,222-224]. For example, CoF of graphene on Ni surface in sliding against fused silica was reported to be as low as 0.03 for ambient conditions [224]. These small scale tribo-contact studies showed a common trend that CoF is increasing with a reduction in a number of monolayers of graphene or *h*-BN, which was explained by out of plane deformations and puckering [222,223]. Such mechanisms occur for thin 2D layers with weak adhesion to substrates and especially pronounced when substrates are not atomically smooth, as predicted with molecular dynamics simulations [225]. In view of these results, it was interesting to observe that in macroscopic tests of steel and copper surfaces covered with graphene flakes a considerable friction reduction was found in all cases, even as the surface roughness was much larger when compared to graphene thickness [226-228]. A review by Berman et al. [67] summarizes reports on the lubrication with graphene, where a stable CoF of about 0.15 against steel counterparts at room temperature is found for both humid air and dry nitrogen environments, which differentiates graphene tribological behavior from that of graphite. As the contact load and number of sliding cycles are increased, graphene disordering and removal are progressing as surface wear mechanisms [67,228].

High temperature friction behavior of 2D materials is yet to be investigated. Initial reports with graphene indicate thermal stability in air up to 500 °C for monolayer and 600 °C for bilayer thicknesses [229], as well as good protection of metal surfaces from oxidation and corrosion [230-233]. These properties of graphene may warrant a benefit for elevated temperature contacts. Recent studies of Ni_3Al self-lubricated composites with embedded graphene flakes had shown a stable CoF of about 0.2 against Si_3N_4 balls from room to 400 °C in air, above which oxidation of graphene flakes leads to CoF increase [234]. High temperature oxidation is a primary concern with both graphene and 2D dichalcogenides. From this perspective, other materials in the 2D family, such as transition metal oxides, perovskites, and their heterostructures with graphene and dichalcogenides [221] remain to be explored for adaptive lubrication concepts at elevated temperatures.

4. Thermal management of solid lubricated contacts

Thermal management of solid tribological contacts in the absence of coolant media, such as oils, defines one of the outstanding challenges for the wider expansion of solid lubrication approaches as discussed in the introduction of this review. One main objective of thermal management of mechanical contacts is to reduce heat spikes and redistribute thermal loading from dry sliding friction to prevent the decomposition or deterioration of the contacts and underlying substrate materials. Modern designs of hard coatings for dry machining tools include thermo barrier considerations as a necessary attribute. Most often this results in multilayer designs by inserting layers with a low thermal conductivity, e.g. adding Al_2O_3 layers [235,236], and employing phonon scattering at the interfaces [237,238]. The interface phonon scattering is an especially powerful approach, as this can create a high degree of thermal anisotropy even if individual layers are relatively good conductors or coatings contain metal inclusions. Recent modeling studies for cathodic arc grown TiN/CrAlN multilayer coatings with metal droplet inclusions indicate that thermal anisotropy for cross-plane and in-plane layer directions approaches a factor of 3 when individual layer thickness is reduced from 2.25 to 0.15 µm [238]. While the studies with multilayer hard coatings show the potential, the adaptive thermal management attribute of high temperature tribological contacts is yet in a relative infancy of development when compared to the progress with improving surface hardness, lubrication, and oxidation stability. Some examples of possible approaches toward adaptive thermal management are schematically shown in Fig. 13 and discussed in this section.

In the self-hardened coating developments for dry machining, it was found that structural evolution in the TiAlN coatings from cubic to a mixed cubic/wurtzite structure is also accompanied by a change in the coating thermal conductivity. This coating had a relatively low thermal conductivity up to 1100 °C due to phonon scattering at grain boundaries for the two-phase structure evolution. At the higher temperature onset of grain coursing, a three-fold increase of thermal conductivity from 3 to about 12 $Wm^{-1}K^{-1}$ was observed [239]. Such a change can enhance thermal load spreading at the sliding contact in the case of the contact overheating. At the same time, it is also possible to block heat propagation when using oxidation resistant amorphous coatings. For example, B-Si-C-N high temperature stable amorphous coatings developed by Vlček et al. [240,241] were shown to maintain thermal conductivity as low as 1.3 $Wm^{-1}K^{-1}$ even after prolonged annealing up to 1400 °C [242]. Such coatings could be used when the protection of the underlying material from the excess temperature is one of the major requirements.

Hexagonal solid structure reorientation discussed earlier for adaptive tribological behavior, also provides remarkable control over the heat flow in the contact zone. Figure 14 shows the effect of the transverse thermal conductivity in MoS_2 hexagonal lubricant, when basal planes are either parallel or perpendicular to the sliding surface and includes amorphous MoS_2 as a reference point [243]. For basal plane orientation parallel to the surface, the measured transverse thermal conductivity is reduced by a factor of four, which is supported by molecular dynamic simulation studies of the heat flow in hexagonal MoS_2 [244,245]. Such thermal conductivity anisotropy is also extended to WS_2 and WSe_2 solid lubricants, which have better thermal oxidation stability as compared to MoS_2. In the case of WSe_2 coatings, the transverse thermal conductivity for (002) orientation was found to be as low as 0.1 $Wm^{-1}K^{-1}$ [245]. This is an order of magnitude lower that of bulk WSe_2. The effect was assigned to the additional phonon scattering modes due to misalignments in hexagonal plane stacking as well as by phonon scattering on grain boundaries and defects. It was also reported that thermal conductivity as low as 0.05 $Wm^{-1}K^{-1}$ (approaching that of air) is achievable in the fully dense turbostratic WSe_2 materials [246]. This creates the opportunity to block heat flow from the contact zone into the underlying coating volume and redirect heat flux parallel to the sliding contact, contributing to the sliding contact thermal management.

An adaptive conversion from a relatively high to a lower thermal conductivity under an exposure to the high temperature is also possible. For example, surface oxide developments can provide effective means for adaptive regulation of thermal transport in hard coating surfaces. Recent studies of thermal conductivity in hard oxynitride coatings by Böttger et al. [247] show that thermal conductivity decreases from 9 to 2 $Wm^{-1}K^{-1}$ for $CrN_{1-x}O_x$ and from 35 to 5 $Wm^{-1}K^{-1}$ for $TiN_{1-x}O_x$ coatings when x is increased from 0 to 0.5. The coating thermal oxidation can be then used to block thermal flow into substrate. In another example, a self-lubricating YSZ-Ag high temperature tribological coating was shown by Gengler et al. [248] to reduce thermal conductivity by a factor of 5 at the exposure to 500 °C for an hour in air, which essentially changed this coating from a moderate heat spreader to a good thermal insulator with an about 1.6 $Wm^{-1}K^{-1}$ thermal conductivity. The mechanism behind such thermal conductivity reduction was an opening nanoscopic size voids in the coating structure when silver was diffused to the surface, similar as it is seen in Figure 3b for a CrN-Ag adaptive coating. This mechanism is irreversible, and can be used as limiter protection for an accidental exposure to a high temperature spike.

Reversible mitigation of thermal spikes can be achieved by employing contained melting/solidification cycle to exploit the latent heat associated with phase transitions for short-term thermal energy storage and temperature averaging in the contact [249]. This concept is yet to be advanced in the practice of the high temperature solid lubrication. Initial studies with the differential scanning calorimetry (DSC) experiments for V_2O_5 phase based lubrication of adaptive TiAlN-VN coatings point that such is possible for the sliding contact zone thermal control [250]. Phase change based thermal management of siding contacts was also studied by Jantschner et al. [251] for vanadium alloyed ZrO_2 adaptive hard coatings. Figure 15 shows the example of DSC studies of the heat consumption and release during phase transitions of a ZrO_2-V coating. This adaptive coating formed a ZrV_2O_7 phase at 600 °C, which was then decomposed above 740 °C into ZrO_2 and liquid V_2O_5, decreasing CoF in sliding against alumina balls to below 0.2 at 800 °C. The endothermic melting of the V_2O_5 observed at 680 °C can be used to mitigate local flash temperatures for heavily loaded sliding contacts. However, the heat of the observed endothermic reaction is low and additional development and surface engineering are required to advance such phase change concept for adaptive contact thermal management.

5. *In situ* methods for investigating the high temperature adaptive lubrication mechanisms

As highlighted in the previous sections, high temperature sliding induces complex chemical and structural evolution of contact surfaces and underlying material volumes. The successful development of wear protective hard coatings with temperature adaptive solid lubrication is critically dependent on the ability to capture and understand these compositional and microstructural evolutions in real time. *In situ* methods of tribological contact investigations received a significant attention in the modern era of tribology science. Such methods include: surface force apparatus [252-254], scanning tunneling probe microscopy [255,256], atomic force microscopy [257-264], quartz crystal microbalance [265-267], contact resistance measurements [268,269], microelectromechanical system testing platforms [270-274], Kelvin probe measurements [275,276], optical characterization with Raman spectroscopy [277-283], optical interferometry [129,284,285], infra-red (IR) spectroscopy [286,287], Auger and x-ray photoelectron spectroscopy [288,289], surface plasmon resonance combined with surface enhanced Raman spectroscopy [290], scanning electron microscopy [106,291], transmission electron microscopy [128,292-294], IR imaging of the contact surfaces [295], and the list is continuing to grow. Some of these *in situ* tribological investigation approaches were reviewed by Wahl and Sawyer [296].

All of the *in situ* tribological contact investigation methods mentioned above are used at relatively moderate contact temperatures and some at cryogenic temperatures. The existing literature for high temperature tribological investigations typically provides friction measurements with post-test analysis of worn surfaces, as temperature and oxidative environments severely interfere with the *in situ* instrumentation. To counteract this challenge, special design arrangements are needed for high temperature sliding contact interrogations. A unique test arrangement was developed by USA AFRL scientists when using Raman spectroscopy to observe evolution of adaptive chameleon hard coatings for sliding temperatures up to 1000 °C [297]. To the extent of the authors' knowledge this is the only reported high temperature friction test apparatus with *in situ* chemistry and structural characterization in air. The apparatus was built using a typical pin-on-disk test setting, where an excitation laser beam and return signal are routed to the contact surface through a guiding tube inserted into high temperature cell, surrounding the sliding contact arrangement. The guiding tube is continuously flooded with cold nitrogen

gas to avoid distortions within the optical assembly. Automated control over the Raman spectroscopy signal guide allowed the spectra to be sampled in the wear track immediately after pin contact or in the surface regions adjacent to the wear track.

One example that shows the necessity to use *in situ* characterization of chemistry and structure of the wear surfaces is shown in Figure 16 (a). This figure compares Raman spectra taken from the VN-Ag adaptive coating wear track location during sliding against Si_3N_4 ball at 700 °C and at the same location shortly after the test termination and cooling to 350 °C prior to the sample extraction for post-test analysis [60,297]. One clearly observes a dramatic difference in the Raman spectra during sliding and after cooling to moderate temperature. What was important to the study of these adaptive VN-Ag coatings, is that Ag_3VO_4 and $AgVO_3$ phases were present at cooling to 350 °C, but only the high silver content Ag_3VO_4 phase was present during the sliding at 700 °C. The high silver content oxide phase was associated with the observed stable CoF of about 0.2 at this high temperature test. In the discussions of the broad temperature range adaptive coatings of this review, it was noted that sulfur from MoS_2 additives for low temperature lubrication is aslo acting as catalyst toward a formation of high temperature lubricious ternary oxides [56]. The *in situ* high temperature Raman spectroscopy arrangement helped to verify this. Figure 16(b) compares *in situ* Raman spectra for an adaptive NbN-Ag made with and without MoS_2 additions [61]. A formation of Ag_2MoO_7 inside the wear track at 700 °C is clearly observed, which is not present for the coatings without MoS_2 addition. This difference was correlated with the lubricious nature of this ternary oxide and CoF reduction to below 0.1. *In situ* Raman spectroscopy tool was hence essential for identifying adaptive lubrication mechanisms for this coating, which had CoF of about 0.1-0.2 in sliding against Si_3N_4 balls from room to 1000 °C [61]. *In situ* Raman spectroscopy discoveries of oxide phases in the wear tracks at different temperature regimes were facilitated by modeling of layered oxides [59]. Integration of these two methods helped to quickly yield multiple nitride based coating compositions for adaptive high temperature lubrication with ternary oxides, including molybdates [51,56-59], vanadates [60], tungstates [59], niobates [61], and tantalates [62].

There still a significant gap in available *in situ* methods for high temperature tribology, when compared to the multitude of moderate temperature diagnostics for surface chemistry, structure, and morphology. From the perspective of surviving high temperature oxidative environments, methods with non-contact arrangements such as spectroscopy and microscopy would likely be a primary choice. Even for such non-contact arrangements the attention to the involved access ports of the high temperature test cells, focusing lenses, signal guides to the detector, etc. are some of the challenges to overcome. Spectroscopic methods are especially of interest as they carry information about both chemical and structural evolution in high temperature tests. Overall, the future of high-temperature adaptive coatings with reduced friction coefficients over a broad temperature range is directly tied to the development of *in situ* investigation methods. This is also linked with advanced modeling to accelerate identification and exploration of adaptive lubrication mechanisms.

6. Conclusions

Hard coating advancements have evolved significantly - from mainly high hardness coatings to current coatings with multifaceted functionalities of high hardness, toughness, temperature stability, oxidation resistance, low friction and wear. Considerable progress has been made in identifying and exploring adaptive mechanisms to enable broad temperature solid lubrication of hard coatings. Environment-

assisted oxidation to form easy to shear and low melting point Magnéli and double oxides, temperature activated metal lubricant diffusion, and thermo-mechanically induced phase transitions to reorient hexagonal solids and promote surface self-hardening are the primary adaptive mechanisms. Together, these can be combined to cover temperature ranges from room to 1000 °C through complex, environment and counterpart dependent evolutions of chemistry, morphology, and compositions. The reversibility in the adaptive coating behavior at temperature cycling remains one of the main challenges, where progress was made using a combination of solid lubricant diffusion control and isolation from the oxidizing environment until its presence is necessary at the mechanical contact area.

For wider application of hard low friction coatings in machinery components, the functionality of contact thermal management is needed. Comparable to other hard coating attributes, this functionality is not well developed and therefore creates both challenge and opportunity for adaptive coating designers. Some of the approaches for adaptive regulation of coating thermal conductivity, heat flow, and thermal spike mitigations are identified when using structural evolution and phase transition mechanisms in hard coatings. These are promising, but yet are very early in the exploration. The addition of thermal management to high temperature hard coatings functionalities can lead to a paradigm extension of solid lubricated hard coatings in machinery components, where oil and coolant technologies currently prevail.

New adaptive mechanisms are also actively sought where the progress via *ab initio* modeling of intrinsically layered solids, such as MAX phases and similar, point to possible new compositions for thermally stable and easy-to-shear adaptive coatings. However, many challenges remain for their practical realization due to the need for tight structural and compositional control in their synthesis. Load and temperature adaptive tribological surfaces are also possible with arrays of compliant nanotube materials. CNT and BNNT array infiltration with solid lubricants can add to the low friction coefficients, increase surface durability for sliding in oxidizing environment, and extend the boundaries of high temperature operation for such compliant coating surfaces. 2D materials with intrinsically low shear and inert surfaces may provide another opportunity for future adaptive lubrication, especially if their temperature stability can be improved, as for example with 2D oxides or heterostructures of oxides with dichalcogenides and graphene.

The progress with temperature adaptive hard coatings with solid lubrication and thermal management functions for robust operations at elevated temperatures and thermal cycling critically depends on the development of *in situ* techniques to identify contact surface phase and structural evolutions at different temperature regimes. While a multitude of such methods exist for low temperatures, high temperature *in situ* investigation methods are very limited. When realized and combined with predictive modeling techniques, they will significantly accelerate the next generation adaptive coating developments. This was confirmed with an example of *in situ* Raman spectroscopy use for realization of a broad temperature range adaptive hard coatings.

Acknowledgments

Professor J. M. Schneider of RWTH Aachen University is acknowledged for valuable comments. The authors acknowledge the Air Force Office of Scientific Research (AFOSR) for the continued financial support. AV and CM acknowledge support from Tribology in Extreme Environments, Thermal Sciences, and Aerospace Materials for Extreme Environments programs of AFOSR. SA acknowledges AFOSR award No. FA9550-12-1-0221.

References

[1] Lubricant Oil Manufacturing in the US: Market Research Report, IBISWorld. 6-17-2013. http://www.prweb.com/releases/2013/6/prweb10835562.htm

[2] O. Knotek, M. Bohmer, T. Leyendecker, J.Vac.Sci.Technol.A 4 (1986) 2695.

[3] I. Petrov, L. Hultman, J. E. Sundgren, J. E. Greene, J.Vac.Sci.Technol.A 10 (1992) 265.

[4] J. E. Sundgren, Thin Solid Films 128 (1985) 21.

[5] H. Holleck, J.Vac.Sci.Technol.A 4 (1986) 2661.

[6] W. D. Sproul, J.Vac.Sci.Technol.A 12 (1994) 1595.

[7] J. Musil, Surf.Coat.Technol. 125 (2000) 322.

[8] A. Matthews, A. Leyland, Heat Treatment of Metals 28 (2001) 63.

[9] S. Veprek, A. S. Argon, J.Vac.Sci.Technol.B 20 (2002) 650.

[10] P. E. Hovsepian, W. D. Munz, Vacuum 69 (2002) 27.

[11] C. Mitterer, P. H. Mayrhofer, J. Musil, Vacuum 71 (2003) 279.

[12] P. H. Mayrhofer, C. Mitterer, L. Hultman, H. Clements, Progr.Mater.Sci. 51 (2006) 1032.

[13] A. Raveh, I. Zukerman, R. Shneck, R. Avni, I. Fried, Surf.Coat.Technol. 201 (2007) 6136.

[14] M. Stueber, H. Holleck, H. Leiste, K. Seemann, S. Ulrich, C. Ziebert, Journal of Alloys and Compounds 483 (2009) 321.

[15] J. Musil, Surf.Coat.Technol. 207 (2012) 50.

[16] D. McIntyre, J. E. Greene, G. Hakansson, J. E. Sundgren, W. D. Munz, J.Appl.Phys. 67 (1990) 1542.

[17] S. Veprek, S. Reiprich, Thin Solid Films 268 (1995) 64.

[18] F. Vaz, L. Rebouta, M. Andritschky, M. F. da Silva, J. C. Soares, Surf.Coat.Technol. 98 (1998) 912.

[19] C. Rebholz, J. M. Schneider, A. A. Voevodin, J. Steinebrunner, C. Charitidis, S. Logothetidis, A. Leyland, A. Matthews, Surf.Coat.Technol. 113 (1999) 126.

[20] C. Mitterer, P. Losbichler, F. Hofer, M. Beschliesser, P. Warbichler, P. N. Gibson, W. Gissler, Vacuum 50 (1998) 313.

[21] S. Carvalho, L. Rebouta, E. Ribeiro, F. Vaz, M. F. Denannot, J. Pacaud, J. P. Rivière, F. Paumier, R. J. Gaboriaud, E. Alves, Surf.Coat.Technol. 177-178 (2004) 369.

[22] D. V. Shtansky, A. N. Sheveiko, M. I. Petrzhik, F. V. Kiryukhantsev-Korneev, E. A. Levashov, A. Leyland, A. L. Yerokhin, A. Matthews, Surf.Coat.Technol. 200 (2005) 208.

[23] M. Pfeiler, J. Zechner, M. Penoy, C. Michotte, C. Mitterer, M. Kathrein, Surf.Coat.Technol. 203 (2009) 3104.

[24] H. Paschke, M. Stueber, C. Ziebert, M. Bistron, P. Mayrhofer, Surf.Coat.Technol. 205 (2011) S24-S28.

[25] A. Erdemir, Tribology Letters 8 (2000) 97.

[26] K. Kutschej, P. H. Mayrhofer, M. Kathrein, P. Polcik, C. Mitterer, Surf.Coat.Technol. 188-189 (2004) 358.

[27] P. E. Hovsepian, D. B. Lewis, Q. Luo, W.-D. Münz, P. H. Mayrhofer, C. Mitterer, Z. Zhou, W. M. Rainforth, Thin Solid Films 485 (2005) 160.

[28] G. Gassner, P. H. Mayrhofer, K. Kutschej, C. Mitterer, M. Kathrein, Surf.Coat.Technol. 201 (2006) 3335.

[29] R. Franz, C. Mitterer, Surf.Coat.Technol. 228 (2013) 1.

[30] A. Erdemir, Tribology International 38 (2005) 249.

[31] A. A. Voevodin, J. S. Zabinski, C. Muratore, Tsinghua Science and Technology 10 (2005) 665.

[32] T. Polcar, A. Nossa, M. Evaristo, A. Cavaleiro, Reviews on Advanced Materials Science 15 (2007) 118.

[33] C. Muratore, A. A. Voevodin, Annual Reviews of Materials Research 39 (2009) 11.1-11.28.

[34] S. M. Aouadi, B. Luster, P. Kohli, C. Muratore, A. A. Voevodin, Surf.Coat.Technol. 204 (2009) 962.

[35] S. Gupta, M. W. Barsoum, Wear 271 (2011) 1878.

[36] T. W. Scharf, S. V. Prasad, Journal of Materials Science 48 (2013) 511.

[37] A. Matthews, S. Franklin, K. Holmberg, J Phys D 40 (2007) 5463.

[38] H. E. Sliney, Thin Solid Films 64 (1979) 211.

[39] H. E. Sliney, Tribol.International October (1982) 303.

[40] C. DellaCorte, Surf.Coat.Technol. 86-87 (1996) 486.

[41] C. DellaCorte, J. A. Fellenstein, Tribology Transactions 40 (1997) 639.

[42] C. DellaCorte, Tribology Transactions 43 (2000) 257.

[43] E. E. Balic, T. A. Blanchet, Wear 259 (2005) 876.

[44] J. S. Zabinski, M. S. Donley, V. J. Dyhouse, N. T. McDevit, Thin Solid Films 214 (1992) 156.

[45] J. S. Zabinski, M. S. Donley, N. T. McDevit, Wear 165 (1993) 103.

[46] M. S. Donley, J. S. Zabinski, Tribological Coatings, in: D. B. Chrisey, G. K. Hubler (Eds.), Pulsed Laser Deposition of Thin Films, John Wiley and Sons, New York, 1994, pp. 431-454.

[47] J. S. Zabinski, A. E. Day, M. S. Donley, C. DellaCorte, N. T. McDevitt, Journal of Materials Science 29 (1994) 5875.

[48] P. J. John, S. V. Prasad, A. A. Voevodin, J. S. Zabinski, Wear 219 (1998) 155.

[49] A. A. Voevodin, J. J. Hu, T. A. Fitz, J. S. Zabinski, Surf.Coat.Technol. 146-147 (2001) 351.

[50] C. Muratore, A. A. Voevodin, J. J. Hu, J. G. Jones, J. S. Zabinski, Surf.Coat.Technol. 200 (2005) 1549.

[51] C. Muratore, A. A. Voevodin, J. J. Hu, J. S. Zabinski, Wear 261 (2006) 797.

[52] J. J. Hu, C. Muratore, A. A. Voevodin, Composite Science and Technology 67 (2007) 336.

[53] C. Muratore, J. J. Hu, A. A. Voevodin, Thin Solid Films 515 (2007) 3638.

[54] C. Muratore, J. J. Hu, A. A. Voevodin, Surf.Coat.Technol. 203 (2009) 957.

[55] A. A. Voevodin, J. J. Hu, T. A. Fitz, J. S. Zabinski, J.Vac.Sci.Technol.A 20 (2002) 1434.

[56] C. Muratore, A. A. Voevodin, Surf.Coat.Technol. 201 (2006) 4125.

[57] S. M. Aouadi, Y. Paudel, B. Luster, S. Stadler, C. Muratore, C. Hager, A. A. Voevodin, Tribol.Lett. 29 (2008) 95.

[58] S. M. Aouadi, Y. Paudel, W. J. Simonson, Q. Ge, P. Kohli, C. Muratore, A. A. Voevodin, Surf.Coat.Technol. 203 (2009) 1304.

[59] D. Stone, J. Liu, D. P. Singh, C. Muratore, A. A. Voevodin, S. Mishra, C. Rebholz, Q. Geb, S. M. Aouadi, Scripta Materialia 62 (2010) 735.

[60] S. M. Aouadi, D. P. Singh, D. S. Stone, K. Polychronopoulou, K. Nahif, C. Rebholz, C. Muratore, A. A. Voevodin, Acta Materialia 58 (2010) 5326.

[61] D. S. Stone, J. Migas, A. Martini, T. Smith, C. Muratore, A. A. Voevodin, S. M. Aouadi, Surf.Coat.Technol. 206 (2012) 4316.

[62] D. S. Stone, S. Harbin, H. Mohseni, J. E. Mogonye, T. W. Scharf, C. Muratore, A. A. Voevodin, A. Martini, S. M. Aouadi, Surf.Coat.Technol. 217 (2013) 140.

[63] X. Zhang, B. Luster, A. Church, C. Muratore, A. A. Voevodin, P. Kohli, S. M. Aouadi, S. Talapatra, Applied Materials and Interfaces 1 (2009) 735.

[64] S. Gupta, D. Filimonov, T. Palanisamy, T. El-Raghy, M. W. Barsoum, Wear 262 (2007) 1479.

[65] S. Gupta, D. Filimonov, V. Zaitsev, T. Palanisamy, M. W. Barsoum, Wear 264 (2008) 270.

[66] S. Gupta, D. Filimonov, T. Palanisamy, M. W. Barsoum, Wear 265 (2008) 560.

[67] D. Berman, A. Erdemir, A. V. Sumant, Mater.Today 17 (2014) 31.

[68] A. A. Voevodin, J. P. O'Neill, J. S. Zabinski, Tribol.Lett. 6 (1999) 75.

[69] A. A. Voevodin, J. S. Zabinski, Thin Solid Films 370 (2000) 223.

[70] A. A. Voevodin, J. S. Zabinski, Composites Science and Technology 65 (2005) 741.

[71] A. A. Voevodin, M. A. Capano, S. J. P. Laube, M. S. Donley, J. S. Zabinski, Thin Solid Films 298 (1997) 107.

[72] A. A. Voevodin, J. S. Zabinski, J.Mater.Sci. 33 (1998) 319.

[73] A. A. Voevodin, C. Muratore, J. S. Zabinski, Chameleon or Smart Solid Lubricating Coatings, in: Q. J. Wang, Y. W. Chung (Eds.), Encyclopedia of Tribology, Springer, 2013, pp. 347-354.

[74] M. R. Hilton, P. D. Fleischauer, Surf.Coat.Technol. 54/55 (1992) 435.

[75] F. P. Bowden and D. Tabor, The Friction and Lubrication of Solids, Oxford, New York, 1986, pp. 81-85.

[76] T. Spalvins, J.Vac.Sci.Technol.A 5 (1987) 212.

[77] R. D. Arnell, A. Soliman, Thin Solid Films 53 (1978) 333.

[78] H. E. Sliney, ASLE Trans. 29 (1985) 370.

[79] A. A. Voevodin, J. G. Jones, J. J. Hu, T. A. Fitz, J. S. Zabinski, Thin Solid Films 401 (2001) 187.

[80] J. L. Endrino, J. J. Nainaparampil, J. E. Krzanowski, Surf.Coat.Technol. 157 (2002) 95.

[81] C. P. Mulligan, D. Gall, Surf.Coat.Technol. 200 (2005) 1495.

[82] K. Kutschej, C. Mitterer, C. P. Mulligan, D. Gall, Adv.Engineering Mat. 8 (2006) 1125.

[83] C. P. Mulligan, T. A. Blanchet, D. Gall, Wear 269 (2010) 125.

[84] P. Basnyat, B. Luster, Z. Kertzman, S. Stadler, P. Kohli, S. Aouadi, J. Xu, S. R. Mishra, O. L. Eryilmaz, A. Erdemir, Surf.Coat.Technol. 202 (2007) 1011.

[85] W. Gulbinski, T. Suszko, Surf.Coat.Technol. 201 (2006) 1469.

[86] D. V. Shtansky, A. V. Bondarev, P. V. Kiryukhantsev-Korneev, T. C. Rojas, V. Godinho, A. Fernandez, Applied Surface Science 273 (2013) 408.

[87] J. J. Hu, A. A. Voevodin, J. S. Zabinski, Journal of Materials Research 20 (2005) 1860.

[88] C. P. Mulligan, P. A. Papi, D. Gall, Thin Solid Films 520 (2012) 6774.

[89] P. A. Papi, C. P. Mulligan, D. Gall, Thin Solid Films 524 (2012) 211.

[90] C. Muratore, A. A. Voevodin, J. J. Hu, J. S. Zabinski, Tribol.Lett. 24 (2006) 201.

[91] G. Gassner, P. H. Mayrhofer, K. Kutschej, C. Mitterer, M. Kathrein, Tribology Letters 17 (2004) 751.

[92] T. Suszko, W. Gulbinski, J. Jagielski, Surf.Coat.Technol. 194 (2005) 319.

[93] T. Polcar, A. Cavaleiro, International Journal of Refractory Metals and Hard Materials 28 (2010) 15.

[94] M. B. Peterson, S. F. Murray, J. J. Florek, ASLE Transactions 2 (1959) 225.

[95] A. Magnéli, Acta Crystallographica 6 (1953) 495.

[96] A. Magnéli, B. Blomberg-Hansson, L. Kihlborg, G. Sundkvist, Acta Chemica Scandinavica 9 (1955) 1382.

[97] J. Stringer, Journal of the Less-Common Metals 8 (1965) 1.

[98] L. Fiermans, P. Clauws, W. Lambrecht, L. Vanderbroucke, J. Vennik, Physica Status Solidi A 59 (1980) 485.

[99] H. Katzke, P. Toledano, W. Depmeier, Phys.Rev.B 68 (2003) 024109.

[100] U. Schwingenschlogl, V. Eyert, Annalen der Physik 13 (2004) 475.

[101] G. Andersson, Acta Chemica Scandinavica 8 (1954) 1599.

[102] G. Andersson, Acta Chemica Scandinavica 10 (1956) 623.

[103] R. J. D. Tilley, B. G. Hyde, Journal of Physics and Chemistry of Solids 31 (1970) 1613.

[104] H. A. Wriedt, Bulletin of Alloy Phase Diagrams 10 (1989) 358.

[105] A. Magnéli, B. M. Oughton, Acta Chemica Scandinavica 5 (1951) 581.

[106] M. N. Gardos, H. Hyun-Soo, W. O. Winer, Tribology Transactions 33 (1990) 209.

[107] M. N. Gardos, Tribology Letters 8 (2000) 65.

[108] E. Lugscheider, O. Knotek, S. Barwulf, K. Bobzin, Surf.Coat.Technol. 142-144 (2001) 137.

[109] T. Reeswinkel, D. Music, J. M. Schneider, Journal of Physics-Condensed Matter 21 (2009) 145404.

[110] T. Reeswinkel, D. Music, J. M. Schneider, Journal of Physics-Condensed Matter 22 (2010) 292203.

[111] J. S. Zabinski, S. V. Prasad, N. T. McDevit, Advanced Solid Lubricant Coatings for Aerospace Systems, in: Tribology for Aerospace Systems, Proceedings of NATO Advisory Group of

Aerospace Research and Development (AGARD) Conference on Tribology for Aerospace Systems, Sesimbra, Portugal, May 6-7, 1996, AGARD NATO publication CP 589, printed by Canada Communication Group, Hull, Quebec, 1996, p. 3-1.

[112] S. D. Walck, J. S. Zabinski, N. T. McDevitt, J. E. Bultman, Thin Solid Films 305 (1997) 130.

[113] S. V. Prasad, N. T. McDevitt, J. S. Zabinski, Wear 237 (2000) 186.

[114] W. Gulbinski, T. Suszko, W. Sienicki, B. Warcholinski, Wear 254 (2003) 129.

[115] W. Gulbinski, T. Suszko, Wear 261 (2006) 867.

[116] D. S. Stone, H. Gao, C. Chantharangsi, C. Paksunchai, M. Bischof, D. Jaeger, A. Martini, T. W. Scharf, S. M. Aouadi, Surf.Coat.Technol. 244 (2014) 37.

[117] T. Suszko, W. Gulbinski, J. Jagielski, Surf.Coat.Technol. 200 (2006) 6288.

[118] A. Ozturk, K. V. Ezirmik, K. Kazmanli, M. Urgen, O. L. Eryilmaz, A. Erdemir, Tribology International 41 (2008) 49.

[119] V. Ezirmik, E. Senel, K. Kazmanli, A. Erdemir, M. Ürgen, Surf.Coat.Technol. 202 (2007) 866.

[120] L. Rosado, N. H. Forster, H. K. Trivedi, J. P. King, Tribology Transactions 43 (2000) 489.

[121] K. L. Strong, J. S. Zabinski, Thin Solid Films 406 (2002) 174.

[122] M. R. Hilton, R. Bauer, P. D. Fleischauer, Thin Solid Films 188 (1990) 219.

[123] J. Moser, F. Lèvy, Thin Solid Films 228 (1993) 257.

[124] A. A. Voevodin, A. W. Phelps, M. S. Donley, J. S. Zabinski, Diamond Relat.Mater. 5 (1996) 1264.

[125] Y. Liu, A. Erdemir, E. I. Meletis, Surf.Coat.Technol. 86-87 (1996) 564.

[126] Y. Liu, A. Erdemir, E. I. Meletis, Surf.Coat.Technol. 82 (1996) 48.

[127] K. J. Wahl, D. N. Dunn, I. L. Singer, Wear 230 (1999) 175.

[128] J. J. Hu, R. Wheeler, J. S. Zabinski, P. A. Shade, A. Shiveley, A. A. Voevodin, Tribol.Lett. 32 (2008) 49.

[129] M. A. Hamilton, L. A. Alvarez, N. A. Mauntler, N. A. Argibay, R. Colbert, D. L. Burris, C. Muratore, A. A. Voevodin, S. S. Perry, W. G. Sawyer, Tribol.Lett. 32 (2008) 91.

[130] J. J. Hu, J. E. Bultman, C. Muratore, B. S. Phillips, J. S. Zabinski, A. A. Voevodin, Surf.Coat.Technol. 203 (2009) 2322.

[131] T. W. Scharf, P. G. Kotula, S. V. Prasad, Acta Mater. 58 (2010) 4100.

[132] F. Gustavsson, S. Jacobson, A. Cavaleiro, T. Polcar, Surf.Coat.Technol. 232 (2013) 541.

[133] H. Dimigen, C. P. Klages, Surf.Coat.Technol. 49 (1991) 543.

[134] K. Bewilogua, H. Dimigen, Surf.Coat.Technol. 61 (1993) 144.

[135] H. Sjostrom, L. Hultman, J. E. Sundgren, L. R. Wallenberg, Thin Solid Films 232 (1993) 169.

[136] A. A. Voevodin, C. Rebholz, A. Matthews, Tribol.Trans. 38 (1995) 829.

[137] A. A. Voevodin, S. V. Prasad, J. S. Zabinski, J.Appl.Phys. 82 (1997) 855.

[138] A. A. Voevodin, J. P. O'Neill, J. S. Zabinski, Thin Solid Films 342 (1999) 194.

[139] O. Wanstrand, M. Larsson, P. Hedenqvist, Surf.Coat.Technol. 111 (1999) 247.

[140] O. R. Monteiro, M.-P. Delplancke-Ogletree, I. G. G. Brown, Thin Solid Films 342 (1999) 100.

[141] M. Stuber, H. Leiste, S. Ulrich, H. Holleck, D. Schild, Surf.Coat.Technol. 150 (2002) 218.

[142] T. Zehnder, J. Patscheider, Surf.Coat.Technol. 133-134 (2000) 138.

[143] T. Zehnder, J. Matthey, P. Schwaller, A. Klein, P. A. Steinmann, J. Patscheider, Surf.Coat.Technol. 163-164 (2003) 238.

[144] Y. T. Pei, D. Galvan, J. T. De Hosson, A. Cavaleiro, Surf.Coat.Technol. 198 (2005) 44.

[145] W. Gulbinski, S. Mathur, H. Shen, T. Suszko, A. Gilewicz, B. Warcholinski, Applied Surface Science 239 (2005) 302.

[146] G. Gassner, P. H. Mayrhofer, J. Patscheider, C. Mitterer, Thin Solid Films 515 (2007) 5411.

[147] G. Gassner, J. Patscheider, P. H. Mayrhofer, S. turm, C. Scheu, C. Mitterer, Tribology Letters 27 (2007) 97.

[148] M. Stueber, P. B. Barna, M. C. Simmonds, U. Albers, H. Leiste, C. Ziebert, H. Holleck, A. Kovacs, P. Hovsepian, I. Gee, Thin Solid Films 493 (2005) 104.

[149] M. Stueber, U. Albers, H. Leiste, S. Ulrich, H. Holleck, P. B. Barna, A. Kovacs, P. Hovsepian, I. Gee, Surf.Coat.Technol. 200 (2006) 6162.

[150] Y. Z. Huang, M. Stueber, P. Hovsepian, Applied Surface Science 253 (2006) 2470.

[151] A. A. Voevodin, R. Bantle, A. Matthews, Wear 185 (1995) 151.

[152] A. A. Voevodin, S. D. Walck, J. S. Solomon, P. J. John, D. C. Ingram, J. S. Zabinski, M. S. Donley, J.Vac.Sci.Technol.A 14 (1996) 1927.

[153] H. Liu, A. Tanaka, K. Umeda, Thin Solid Films 346 (1999) 162.

[154] T. Krumpiegl, H. Meerkamm, W. Fruth, C. Schaufler, G. Erkens, H. Bohner, Surf.Coat.Technol. 120-121 (1999) 550.

[155] C. Louro, C. W. Moura, N. Carvalho, M. Stueber, A. Cavaleiro, Diam.Relat.Mater. 20 (2011) 57.

[156] R. Gilmore, M. A. Baker, P. N. Gibson, W. Gissler, Surf.Coat.Technol. 105 (1998) 45.

[157] R. Gilmore, M. A. Baker, P. N. Gibson, W. Gissler, Surf.Coat.Technol. 116-119 (1999) 1127.

[158] S. S. Camargo, A. L. B. Neto, R. A. Santos, F. L. Freire, R. Carius, F. Finger, Diam.Relat.Mater. 7 (1998) 1155.

[159] S. S. Camargo, Jr., R. A. Santos, A. L. B. Neto, R. Carius, F. Finger, Thin Solid Films 332 (1998) 130.

[160] W. J. Wu, M. H. Hon, Surf.Coat.Technol. 111 (1999) 134.

[161] R. K. Y. Fu, Y. F. Mei, M. Y. Fu, C. B. Wei, G. G. Siu, P. K. Chu, W. Y. Cheung, S. P. Wong, Proceedings of the SPIE 5774 (2004) 330.

[162] M. C. Chiu, W. P. Hsieh, W. Y. Ho, D. Y. Wang, F. S. Shieu, Thin Solid Films 476 (2005) 258.

[163] D. Hofmann, S. Kunkel, K. Bewilogua, R. Wittorf, Surf.Coat.Technol. 215 (2013) 357.

[164] H. L. Bai, E. Y. Jiang, Thin Solid Films 353 (1999) 157.

[165] W. Kulisch, C. Popov, L. Zambov, J. Bulir, M. P. Delplancke-Ogletree, J. Lancok, M. Jeliinek, Thin Solid Films 377-378 (2000) 148.

[166] L. Su-Jien, L. Chia-Han, L. Wei-Shun, C. Hua-Chun, C. Hung-Jen, C. Shou-Yi, Thin Solid Films 510 (2006) 125.

[167] Y. S. Zou, Y. F. Wu, R. F. Huang, C. Sun, L. S. Wen, Vacuum 83 (2009) 1406.

[168] Y. W. Bae, W. Y. Lee, T. M. Besmann, C. S. Yust, P. J. Blau, Mater.Sci.Eng.A 209 (1996) 372.

[169] R. Gilmore, M. A. Baker, P. N. Gibson, W. Gissler, M. Stoiber, P. Losbichler, C. Mitterer, Surf.Coat.Technol. 108-109 (1998) 345.

[170] R. Goller, P. Torri, M. A. Baker, R. Gilmore, W. Gissler, Surf.Coat.Technol. 120-121 (1999) 453.

[171] Onate, J. I., Brizuela, M., Garcia-Luis, A., Braceras, I., Viviente, J. L., Gomez-Elvira, J. Improved tribological behaviour of MoS_2 thin solid films alloyed with WC. In: European Space Agency Special Publication (ESA SP) Edition 480, published by ESA SP, Liege, Belgium, 2001, pp. 257-262.

[172] J. I. Onate, M. Brizuela, J. L. Viviente, A. Garcia-Luis, I. Braceras, D. Gonzalez, I. Garmendia, Transactions of the Institute of Metal Finishing 85 (2007) 75.

[173] T. Polcar, A. Cavaleiro, Thin Solid Films 519 (2011) 4037.

[174] T. Polcar, M. Evaristo, M. Stueber, A. Cavaleiro, Wear 266 (2009) 393.

[175] M. Evaristo, T. Polcar, A. Cavaleiro, Plasma Processes and Polymers 6 (2009) S92-S95.

[176] V. Y. Fominski, S. N. Grigoriev, J. P. Celis, R. I. Romanov, V. B. Oshurko, Thin Solid Films 520 (2012) 6476.

[177] S. N. Grigoriev, V. Y. Fominski, R. I. Romanov, A. G. Gnedovets, (2014), Thin Solid Films 556 (2014) 35.

[178] D. V. Shtansky, T. A. Lobova, V. Yu. Fominski, S. A. Kulinich, I. V. Lyasotsky, M. I. Petrshik, E. A. Levashov, J. J. Moore, Surf.Coat.Technol. 183 (2004) 328.

[179] C. C. Baker, J. J. Hu, A. A. Voevodin, Surf.Coat.Technol. 201 (2006) 4224.

[180] C. C. Baker, R. R. Chromik, K. J. Wahl, J. J. Hu, A. A. Voevodin, Thin Solid Films 515 (2007) 6737.

[181] J. J. Hu, J. S. Zabinski, J. E. Bultman, J. H. Sanders, A. A. Voevodin, Crystal Growth and Design 8 (2008) 2603.

[182] C. Mitterer, M. Rauter, P. Rödhammer, Surf.Coat.Technol. 41 (1990) 351.

[183] P. H. Mayrhofer, M. Stoiber, C. Mitterer, Scripta Materialia 53 (2005) 241.

[184] P. H. Mayrhofer, C. Mitterer, J. G. Wen, I. Petrov, J. E. Greene, J.Appl.Phys. 100 (2006) 044301.

[185] P. H. Mayrhofer, A. Horling, L. Karlsson, J. Sjolen, T. Larsson, C. Mitterer, L. Hultman, Applied Physics Letters 83 (2003) 2049.

[186] A. Horling, L. Hultman, M. Oden, J. Sjolen, L. Karlsson, J.Vac.Sci.Technol.A 20 (2002) 1815.

[187] Y. H. Lu, J. P. Wang, Y. G. Shen, Materials Science and Technology 23 (2007) 1243.

[188] A. A. Voevodin, J. P. O'Neill, J. S. Zabinski, Surf.Coat.Technol. 116-119 (1999) 36.

[189] S. Y. Li, J. A. Rodriguez, J. Hrbek, H. H. Huang, G. Q. Xu, Surface Science 395 (1998) 216.

[190] M. T. Lavik, T. M. Medved, G. D. Moore, ASLE Transactions 11 (1968) 44.

[191] M. W. Barsoum, Progress in Solid State Chemistry 28 (2000) 201.

[192] W. Jeitschko, H. Nowotny, Monatshefte für Chemie 98 (1967) 329.

[193] M. W. Barsoum, T. El-Raghy, J.Am.Ceram.Soc. 79 (1996) 1953.

[194] M. W. Barsoum, D. Brodkin, T. El-Raghy, Scripta Materialia 36 (1997) 535.

[195] M. W. Barsoum, T. El-Raghy, Metallurgical and Materials Transactions A 30 (1999) 363.

[196] M. W. Barsoum, T. El-Raghy, Journal of Materials Synthesis and Processing 5 (1997) 197.

[197] S. Myhra, J. W. B. Summers, E. H. Kisi, Materials Letters 39 (1999) 6.

[198] A. Crossley, E. H. Kisi, J. W. B. Summers, S. Myhra, Journal of Physics D 32 (1999) 632.

[199] S. Gupta, D. Filimonov, V. Zaitsev, T. Palanisamy, T. El-Raghy, M. W. Barsoum, Wear 267 (2009) 1490.

[200] D. Music, Z. Sun, R. Ahuja, J. M. Schneider, Phys.Rev.B 73 (2006) 134117.

[201] D. Music, J. M. Schneider, Journal of Materials 59 (2007) 60.

[202] H. Bolvardi, J. Emmerlich, M. T. Baben, D. Music, J. von Appen, R. Dronskowski, J. M. Schneider, Journal of Physics Condensed Matter 25 (2013) 045501.

[203] D. Music, A. Houben, R. Dronskowski, J. M. Schneider, Phys.Rev.B 75 (2007) 174102.

[204] Z. M. Sun, D. Music, R. Ahuja, J. M. Schneider, Journal of Physics Condensed Matter 17 (2005) 7169.

[205] Z. Sun, D. Music, R. Ahuja, S. Li, J. M. Schneider, Phys.Rev.B 70 (2004) 092102.

[206] D. Music, Z. Sun, A. A. Voevodin, J. M. Schneider, Solid State Communications 139 (2006) 139.

[207] D. Music, Z. Sun, A. A. Voevodin, J. M. Schneider, Journal of Physics Condensed Matter 18 (2006) 4389.

[208] J. Emmerlich, D. Music, M. Braun, P. Fayek, F. Munnik, J. M. Schneider, Journal of Physics D 42 (2009) 185406.

[209] A. Erdemir, Boron-Based Solid Nanolubricants and Lubrication Additives Nanolubricants, John Wiley & Sons, Ltd, 2008, pp. 203-223.

[210] P. Eklund, M. Beckers, U. Jansson, H. Högberg, L. Hultman, Thin Solid Films 518 (2010) 1851.

[211] J. Emmerlich, G. Gassner, P. Eklund, H. Högberg, L. Hultman, Wear 264 (2008) 914.

[212] D. V. Shtansky, P. Kiryukhantsev-Korneev, A. N. Sheveyko, B. N. Mavrin, C. Rojas, A. Fernandez, E. A. Levashov, Surf.Coat.Technol. 203 (2009) 3595.

[213] W. Gulbinski, A. Gilewicz, T. Suszko, B. Warcholinski, Z. Kuklinski, Surf.Coat.Technol. 180-181 (2004) 341.

[214] J. J. Hu, J. E. Bultman, S. Patton, J. S. Zabinski, Tribology Letters 16 (2004) 113.

[215] M. Rester, J. Neidhardt, P. Eklund, J. Emmerlich, H. Ljungcrantz, L. Hultman, C. Mitterer, Mater.Sci.Eng.A 429 (2006) 90.

[216] A. H. Church, X. F. Zhang, B. Sirota, P. Kohli, S. M. Aouadi, S. Talapatra, Advanced Science Letters 5 (2012) 188.

[217] J. J. Hu, S. H. Jo, Z. F. Ren, A. A. Voevodin, J. S. Zabinski, Tribol.Lett. 19 (2005) 119.

[218] C. Hsiang-Chih, S. Dogan, M. Volkmann, C. Klinke, E. Riedo, Nanotechnology 23 (2012) 455706.

[219] D. Golberg, P. M. F. Costa, O. Lourie, M. Mitome, B. Xuedong, K. Kurashima, Z. Chunyi, T. Chengchun, Y. Bando, Nano Letters 7 (2007) 2146.

[220] A. Skopp, M. Woydt, K.-H. Habig, Wear 181-183, Part 2 (1995) 571.

[221] A. K. Geim, I. V. Grigorieva, Nature 499 (2013) 419.

[222] L. Changgu, L. Qunyang, W. Kalb, L. Xin-Zhou, H. Berger, R. W. Carpick, J. Hone, Science 328 (2010) 76.

[223] Q. Li, C. Lee, R. W. Carpick, J. Hone, Physica Status Solidi B 247 (2010) 2909.

[224] K. S. Kim, H. J. Lee, C. Lee, S. K. Lee, H. Jang, J. H. Ahn, J. H. Kim, H. J. Lee, ACS Nano 5 (2011) 5107.

[225] Y. Dong, J Phys D 47 (2014).

[226] D. Berman, A. Erdemir, A. V. Sumant, Carbon 54 (2013) 454.

[227] D. Berman, A. Erdemir, A. V. Sumant, Carbon 59 (2013) 167.

[228] W. Moon-Sub, O. V. Penkov, K. Dae-Eun, Carbon 54 (2013) 472.

[229] H. Y. Nan, Z. H. Ni, J. Wang, Z. Zafar, Z. X. Shi, Y. Y. Wang, J.Raman Spectrosc. 44 (2013) 1018.

[230] S. Chen, L. Brown, M. Levendorf, W. Cai, S. Y. Ju, J. Edgeworth, X. Li, C. W. Magnuson, A. Velamakanni, R. D. Piner, J. Kang, J. Park, R. S. Ruoff, ACS Nano 5 (2011) 1321.

[231] N. T. Kirkland, T. Schiller, N. Medhekar, N. Birbilis, Corrosion Science 56 (2012) 1.

[232] D. Prasai, J. C. Tuberquia, R. R. Harl, G. K. Jennings, K. I. Bolotin, ACS Nano 6 (2012) 1102.

[233] A. S. Kousalya, A. Kumar, R. Paul, D. Zemlyanov, T. S. Fisher, Corrosion Science 69 (2013) 5.

[234] W. Zhai, X. Shi, M. Wang, Z. Xu, J. Yao, S. Song, Y. Wang, Wear 310 (2014) 33.

[235] W. Grzesik, Wear 240 (2000) 9.

[236] W. Grzesik, P. Nieslony, Journal of Manufacturing Science and Engineering 125 (2003) 689.

[237] L. Braginsky, A. Gusarov, V. Shklover, Surf.Coat.Technol. 204 (2009) 629.

[238] P. H. M. Böttger, A. V. Gusarov, V. Shklover, J. Patscheider, M. Sobiech, International Journal of Thermal Sciences 77 (2014) 75.

[239] R. Rachbauer, J. J. Gengler, A. A. Voevodin, K. Resch, P. Mayrhofer, Acta Materialia 60 (2012) 2091.

[240] J. Kalaš, R. Vernhes, S. Hreben, J. Vlcek, J. E. Klemberg-Sapieha, L. Martinu, Thin Solid Films 518 (2009) 174.

[241] J. Vlcek, S. Hreben, J. Kalaš, J. Capek, P. Zeman, R. Cerstvy, V. Perina, Y. Setsuhara, J.Vac.Sci.Technol.A 26 (2008) 1101.

[242] J. J. Gengler, J. Hu, J. G. Jones, A. A. Voevodin, P. Steidel, J. Vlcek, Surf.Coat.Technol. 206 (2011) 2030.

[243] C. Muratore, V. Varshney, J. J. Gengler, J. Hu, J. E. Bultman, A. K. Roy, B. L. Farmer, A. A. Voevodin, Phys.Chem.Chem.Phys. 16 (2014) 1008.

[244] V. Varshney, S. S. Patnaik, C. Muratore, A. Roy, A. A. Voevodin, Computational Materials Science 48 (2010) 101.

[245] C. Muratore, V. Varshney, J. J. Gengler, J. J. Hu, J. E. Bultman, T. M. Smith, P. J. Shamberger, B. Qiu, X. Ruan, A. K. Roy, A. A. Voevodin, Appl.Phys.Lett. 102 (2013) 081604.

[246] C. Chiritescu, D. G. Cahill, N. Nguyen, D. Johnson, A. Bodapati, P. Keblinski, P. Zschack, Science 315 (2007) 351.

[247] P. H. M. Böttger, E. Lewin, J. Patscheider, V. Shklover, D. G. Cahill, R. Ghisleni, M. Sobiech, Thin Solid Films 549 (2013) 232.

[248] J. J. Gengler, C. Muratore, A. Roy, J. Hu, A. A. Voevodin, S. Roy, J. R. Gord, Composite Science and Technology 14 (2010) 2117.

[249] C. Muratore, S. M. Aouadi, A. A. Voevodin, Surf.Coat.Technol. 206 (2012) 4828.

[250] P. H. Mayrhofer, P. E. Hovsepian, C. Mitterer, W.-D. Münz, Surf.Coat.Technol. 177-178 (2004) 341.

[251] O. Jantschner, C. Walter, C. Muratore, A. A. Voevodin, C. Mitterer, Surf.Coat.Technol. 228 (2013) 76.

[252] D. Tabor, R. H. S. Winterton, Proceedings of the Royal Society of London.A.Mathematical and Physical Sciences 312 (1969) 435.

[253] J. N. Israelachvili, D. Tabor, Proceedings of the Royal Society of London.A.Mathematical and Physical Sciences 331 (1972) 19.

[254] J. Israelachvili, Y. Min, M. Akbulut, A. Alig, G. Carver, W. Greene, K. Kristiansen, E. Meyer, N. Pesika, K. Rosenberg, H. Zeng, Reports on Progress in Physics 73 (2010) 036601.

[255] G. Binnig, C. F. Quate, C. Gerber, Physical Review Letters 56 (1986) 930.

[256] C. M. Mate, R. Erlandsson, G. M. McClelland, S. Chiang, Surface Science 208 (1989) 473.

[257] C. Mathew Mate, G. M. McClelland, R. Erlandsson, S. Chiang, Physical Review Letters 59 (1987) 1942.

[258] G. Meyer, N. M. Amer, Applied Physics Letters 57 (1990) 2089.

[259] G. S. Blackman, C. M. Mate, M. R. Philpott, Vacuum 41 (1990) 1283.

[260] C. M. Mate, Wear 168 (1993) 17.

[261] C. A. J. Putman, V. Igarashi, R. Kaneko, Applied Physics Letters 66 (1995) 3221.

[262] R. W. Carpick, M. Salmeron, Chemical Reviews 97 (1997) 1163.

[263] I. Szlufarska, M. Chandross, R. W. Carpick, Journal of Physics D 41 (2008) 123001.

[264] C. G. Dunckle, I. B. Altfeder, A. A. Voevodin, J. Jones, J. Krim, P. Taborek, J.Appl.Phys. 107 (2010) 114903.

[265] E. T. Watts, J. Krim, A. Widom, Physical Review B 41 (1990) 3466.

[266] J. Krim, D. H. Solina, R. Chiarello, Physical Review Letters 66 (1991) 181.

[267] J. Krim, Nano Today 2 (2007) 38.

[268] K. J. Wahl, M. Belin, I. L. Singer, Wear 214 (1998) 212.

[269] C. Gao, L. Bredell, D. Kuhlmann-Wilsdorf, D. D. Makel, Wear 162-164, Part A (1993) 480.

[270] D. C. Senft, M. T. Dugger, Proceedings of SPIE 3224 (1997) 31.

[271] S. T. Patton, W. D. Cowan, K. C. Eapen, J. S. Zabinski, Tribology Letters 9 (2000) 199.

[272] B. Bhushan, Proceedings of the Institution of Mechanical Engineers Part J-Journal of Engineering Tribology 215 (2001) 1.

[273] A. V. Desai, M. A. Haque, Tribology Letters 18 (2005) 13.

[274] S. H. Kim, D. B. Asay, M. T. Dugger, Nano Today 2 (2007) 22.

[275] T. Kasai, X. Y. Fu, D. A. Rigney, A. L. Zharin, Wear 225 (1999) 1186.

[276] J.-H. Wu, M. Sanghavi, J. H. Sanders, A. A. Voevodin, J. S. Zabinski, D. A. Rigney, Wear 255 (2003) 859.

[277] G. J. Exarhos, M. S. Donley, "Real-Time Raman Detection of Molecular Changes in Ceramics Undergoing Sliding Friction" *Report No. PNL-SA-14794;* (Compiled and Distributed by the NTIS, U.S. Department of Commerce, Battelle Pacific Northwest Labs., Richland, WA, 1987).

[278] N. T. Mcdevitt, M. S. Donley, J. S. Zabinski, Wear 166 (1993) 65.

[279] S. D. Dvorak, K. J. Wahl, I. L. Singer, Tribology Transactions 45 (2002) 354.

[280] T. W. Scharf, I. L. Singer, Tribology Transactions 45 (2002) 363.

[281] I. L. Singer, S. D. Dvorak, K. J. Wahl, T. W. Scharf, J.Vac.Sci.Technol.A 21 (2003) S232-S240.

[282] R. R. Chromik, C. C. Baker, A. A. Voevodin, K. J. Wahl, Mater.Res.Soc.Symp.Proc. 890 (2006) 275.

[283] R. R. Chromik, C. C. Baker, A. A. Voevodin, K. J. Wahl, Wear 262 (2007) 1239.

[284] K. J. Wahl, R. R. Chromik, G. Y. Lee, Wear 264 (2008) 731.

[285] B. A. Krick, J. R. Vail, B. N. J. Persson, W. G. Sawyer, Tribology Letters 45 (2012) 185.

[286] P. M. Cann, H. A. Spikes, Tribology Letters 19 (2005) 289.

[287] F. Mangolini, A. Rossi, N. D. Spencer, Tribology Letters 45 (2012) 207.

[288] W. A. Glaeser, D. Baer, M. Engelhardt, Wear 162-164 (1993) 132.

[289] J. M. Martin, T. Le Mogne, M. Boehm, C. Grossiord, Tribology International 32 (1999) 617.

[290] B. A. Krick, D. W. Hahn, W. G. Sawyer, Tribology Letters 49 (2013) 95.

[291] B. Murarash, M. Varenberg, Tribology Letters 41 (2011) 319.

[292] A. P. Merkle, L. D. Marks, Appl.Phys.Lett. 90 (2007) 064101-064101-3.

[293] A. P. Merkle, L. D. Marks, Wear 265 (2008) 1864.

[294] L. D. Marks, O. L. Warren, A. M. Minor, A. P. Merkle, Mrs Bulletin 33 (2008) 1168.

[295] K. G. Rowe, A. I. Bennett, B. A. Krick, G. W. Sawyer, Tribology International 62 (2013) 208.

[296] W. G. Sawyer, K. J. Wahl, Mrs Bulletin 33 (2008) 1145.

[297] C. Muratore, J. E. Bultman, S. M. Aouadi, A. A. Voevodin, Wear 270 (2011) 140.

Figure Legends

Figure 1. Schematic representation of a solid lubrication with a chameleon adaptive coating. Reprinted with permission from Ref. [73]. Copyright © 2013, Springer Science+Business Media.

Figure 2. TEM image and selected area diffraction pattern of a YSZ-Ag-Mo adaptive coating, showing a nanocrystalline nature and random distribution of Ag inclusions in YSZ matrix. Reprinted with permission from Ref. [52]. Copyright © 2007, Elsevier.

Figure 3. Metal diffusion to the surface from nanoscale size inclusions in ceramic matrices: a) schematic of Ag or Au diffusion out of an adaptive nitride or oxide matrix hard coating. Adapted from Ref. [52]; b) cross-section (top) and surface (bottom) morphology of a CrN-Ag adaptive hard coating after heating to 650 °C. Reprinted with permission from Ref. [88], copyright © 2012, Elsevier.

Figure 4. Multilayer coating for temperature cycle operations: a) schematic of Ag lubricant delivery to wear scar in a multilayered coating made of YSZ-Ag-Mo and TiN diffusion barrier layers. Reprinted with permission from Ref. [54,90]. Copyright © 2006, Springer Science+Business Media, LLC; b) cross-section TEM image of such multilayer after heating to 500 °C where Ag was depleted from the top YSZ-Ag-Mo layer, but kept under TN diffusion barrier layer; c) friction performance of a 2.8 μm thick coating made of a stack of YSZ-Ag-Mo layers interlayered with TiN diffusion barrier layers during non-interrupted sliding against a Si_3N_4 ball and shown imposed temperature cycling. Reprinted with permission from Ref. [54,90]. Copyright © 2009, Elsevier.

Figure 5. Prediction of easy shear origin for selected Magnéli oxides: a) decohesion energy G (filled circles) and elastic constant C_{44} (open circles) as a function of the distance between the cleaved layers for considered oxides listed in the data legend; and b) an example of electron density calculations in (040) plane for V_2O_5 structure in a projection along [010] axis to show an easy shear (002) plane. Reprinted with permission from Ref. [110]. Copyright © 2010, IOP Publishing. All rights reserved.

Figure 6. Ag_2MoO_4 ternary oxide for high temperature lubrication: a) intrinsically layered structure with blue, green, and red spheres representing Ag, Mo, and O, respectively, where a continuous plane of O-Ag-O atoms with easy shear provides high temperature lubrication; b) example of the silver molybdate oxide morphology formed on the surface of a wear track after 300,000 sliding cycles at 600 °C in air against a Si_3N_4 ball (CoF was at 0.1-0.2 for the entire test duration). Reprinted with permission from Ref. [58]. Copyright © 2009, Elsevier.

Figure 7. BFTEM image of a wear track surface cross-section for a $AgTaO_3$ coating after 10,000 sliding cycles at 750 °C in air against a Si_3N_4 ball (CoF was at 0.06): a) surface and subsurface areas morphology; b) high magnification of the surface area marked with square in image a) with a mechanically mixed layer, which is indexed to consist of $AgTaO_3$ (101) and Ta_2O_5 (001) phases. Reprinted with permission from Ref. [62]. Copyright © 2013, Elsevier.

Figure 8. Example of friction induced crystallization and re-orientation in a Mo-W-S-Se composite coating after 1,000 sliding cycles against a SiC fiber tip at room temperature. Reprinted with permission from Ref. [128]. Copyright © 2008, Springer Science+Business Media, LLC.

Figure 9. Temperature stable MoS_2-$MoTe_2$ nanocomposite coating: a) nanoscale sized MoS_2 particle encapsulated with 2H-$MoTe_2$ shell to prevent from oxidation. Reprinted with permission from Ref. [181]. Copyright © 2008, American Chemical Society; b) examples of a friction trace for sliding against silicon nitride at 450 °C in air and Raman spectra from the wear track for a core-shell MoS_2-$MoTe_2$ nanocomposite coating. Adapted with permission from Ref. [130]. Copyright © 2009, Elsevier.

Figure 10. Averaged friction coefficient for sliding tests of a YSZ-Ag-Mo-MoS_2 nanocomposite coating against Si_3N_4 in air as a function of test temperature with examples of Raman spectra recorded from wear track surfaces after test completions at 300 and 700 °C. Reprinted with permission from Ref. [56]. Copyright © 2006, Elsevier.

Figure 11. A high temperature lubrication double layer adaptive tribofilm formation on the surface of Ta_2AlC-Ag composite: a) schematic of the double-layer tribofilm formed in a contact with a superalloy counterpart. Reprinted with permission from Ref. [35]. Copyright © 2011, Elsevier; b) friction coefficient variation during three cycles of heating and cooling in 26–500 °C temperature range. Black data points represent CoF during heating; red, CoF during cooling; blue, temperature during heating; green, temperature during cooling; black dotted line. Vertical dotted lines – stop and start of tests. Reprinted with permission from Ref. [64]. Copyright © 2007, Elsevier.

Figure 12. *Ab initio* predictions of shear in ternary M_2AlC phases (M = Sc, Y, La, Ti, Zr, Hf, V, Nb, Ta, Cr, Mo, W); a) predicted MAX phase shear modulus in (C_{44}) as a function of the shear modulus of the corresponding binary carbide, where a two-group notion in regard of shear reduction is evident (two trends are notionally shown with straight approximate lines). Reprinted with permission from Ref. [206]. Copyright © 2006, Elsevier; b) stress–strain curve for the shear deformation in Nb_2AlC together with the bond length data for Nb–C and Nb–Al, which predicts that the Nb–Al bonds break at the yield point, allowing for further shear stress reduction. Reprinted with permission from Ref. [207]. Copyright © 2006, IOP Publishing. All rights reserved.

Figure 13. Schematic representation of a broad temperature range operation hard protective coating, where adaptive self-lubrication in broad temperature ranges is accompanied by contact thermal management: thermal spike mitigation with a latent heat of melting, lateral heat spreading in self-formed tribofilm, cooling by high surface emissivity, heat flow blocking to substrate by a low thermal conductive coating composition.

Figure 14. Dependence of the cross-thickness thermal conductivity in hexagonal MoS_2 lubricating films as a function of the (002) basal plane preferred orientation. A thermal conductivity measured for an amorphous film is also shown as a reference. Figure is based on data in Ref. [243].

Figure 15. Example of a heat flow in the ZrO_2-V coating material studies by DSC method (coating was removed from the substrate for the study), which shows a strong endothermic peak associated with the V_2O_5 phase melting at heating. The data was taken during second heating-cooling cycling to reduce

influence of irreversible phase transitions at the initial heating. Reprinted with permission from Ref. [251]. Copyright © 2013, Elsevier.

Figure 16. Examples of Raman spectra taken *in situ* from wear tracks in high temperature sliding of hard adaptive coatings against Si_3N_4 balls in air: a) during the sliding tests of an VN-Ag adaptive coating at 700 °C and immediately after test termination and cooling to 350 °C. Adapted with permission from Ref. [60,297]. Copyright © 2010, Elsevier; b) during 700 °C sliding tests of an NbN-Ag adaptive coating with and without MoS_2 additions. Reprinted with permission from Ref. [61]. Copyright © 2012, Elsevier.

Submitted for publication in Surface and Coatings Technology

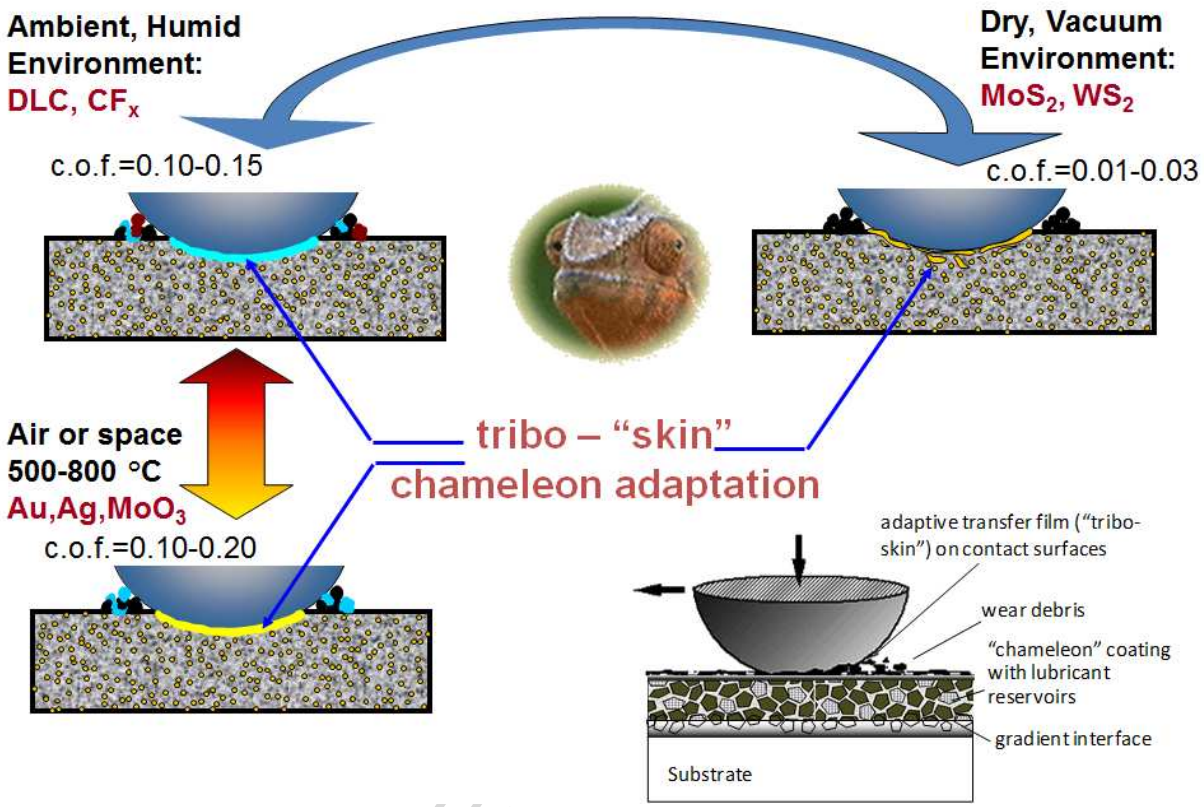

Figure 1

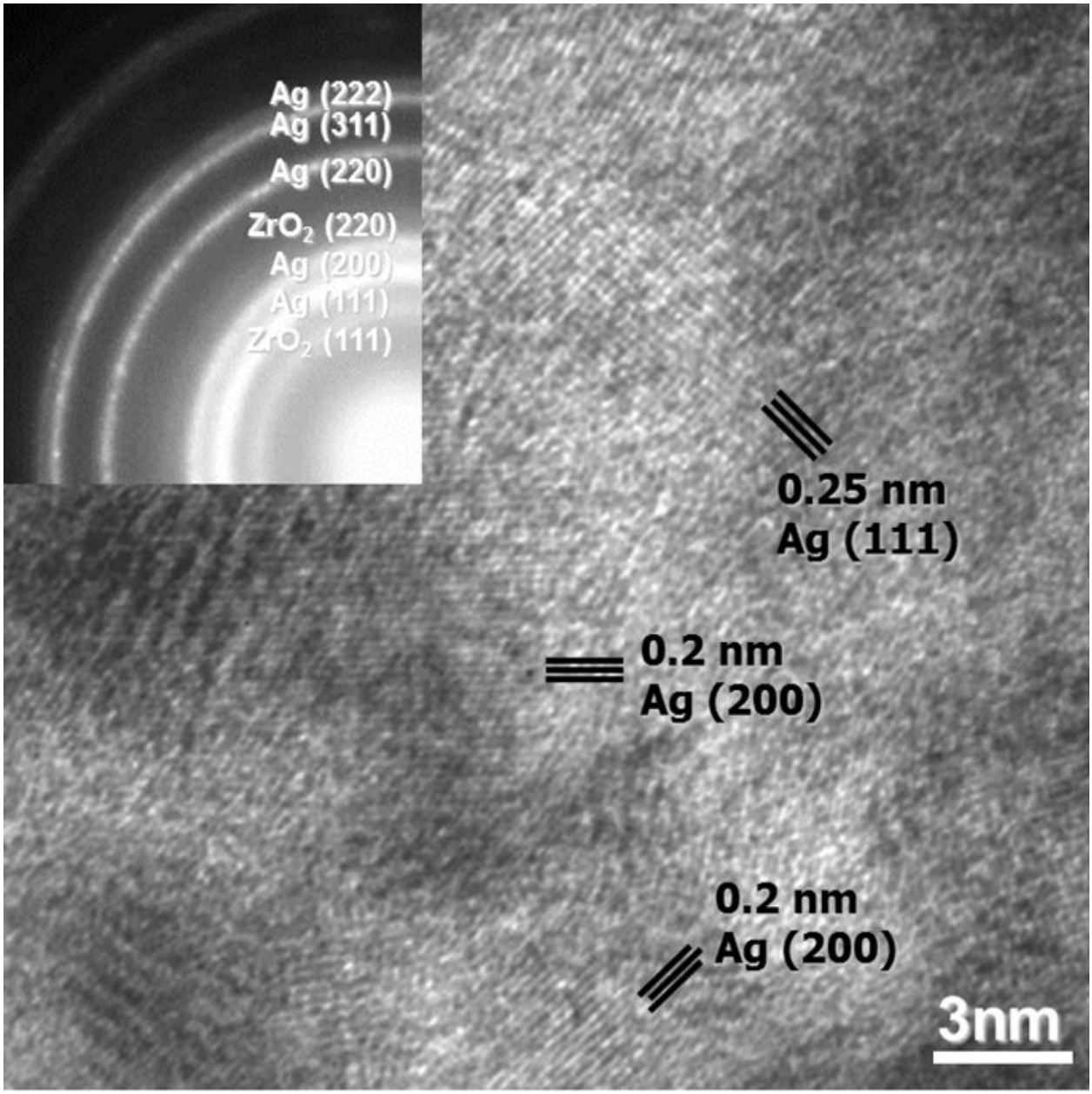
Ag (222)
Ag (311)
Ag (220)
ZrO_2 (220)
Ag (200)
Ag (111)
ZrO_2 (111)
0.25 nm
Ag (111)
0.2 nm
Ag (200)
0.2 nm
Ag (200)
3nm

Figure 2

Submitted for publication in Surface and Coatings Technology

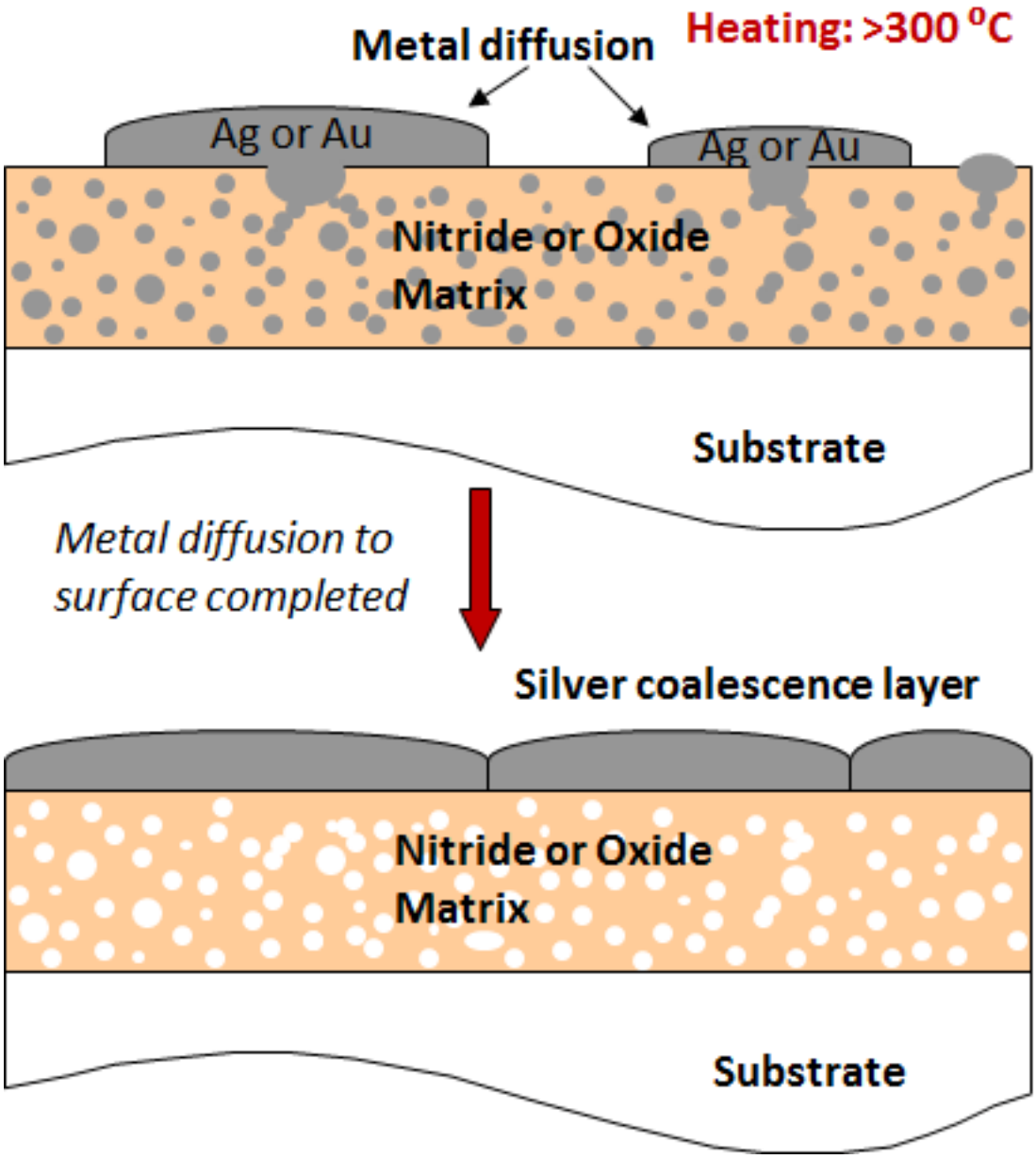

Figure 3a

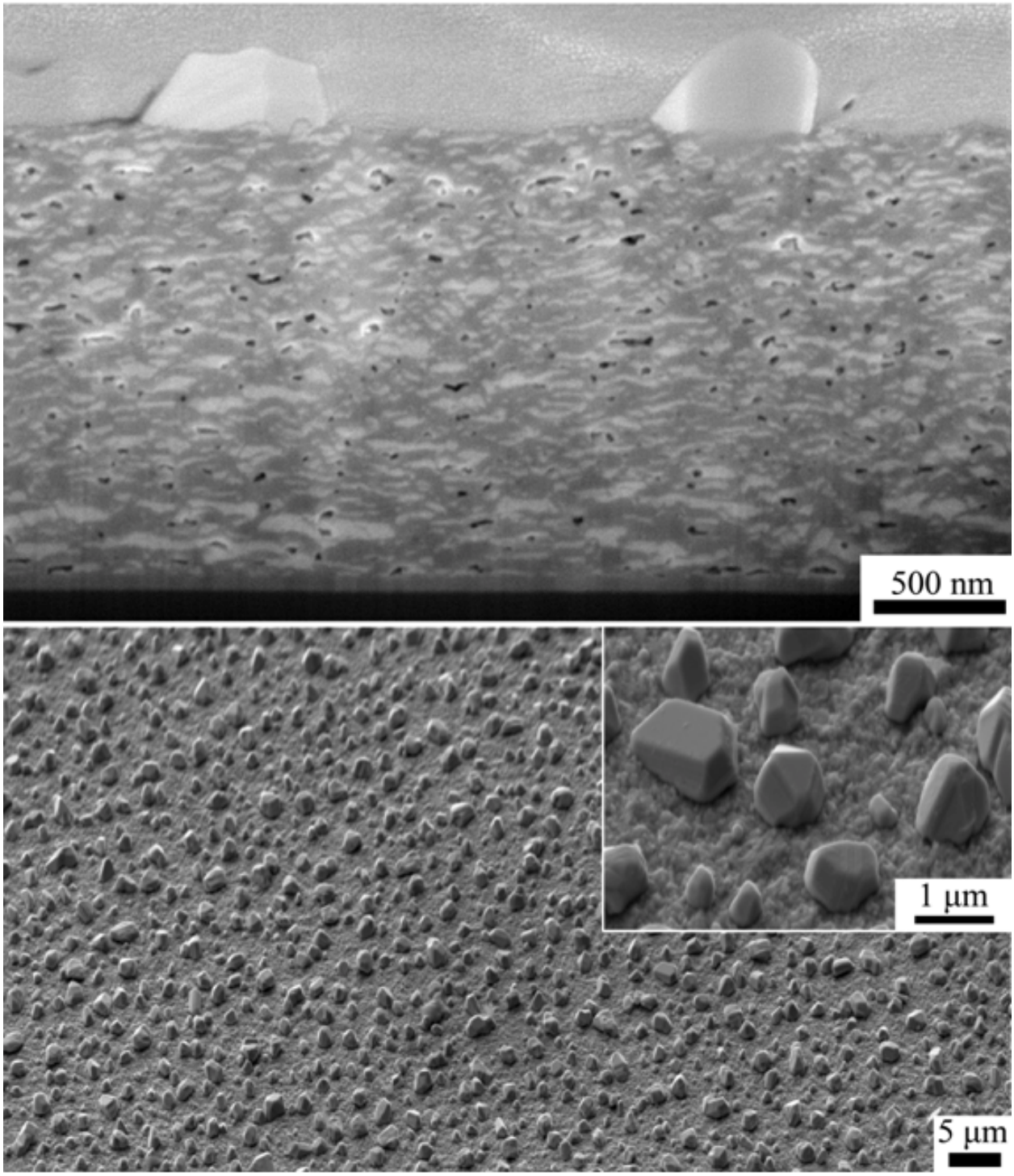

Figure 3b

Submitted for publication in Surface and Coatings Technology

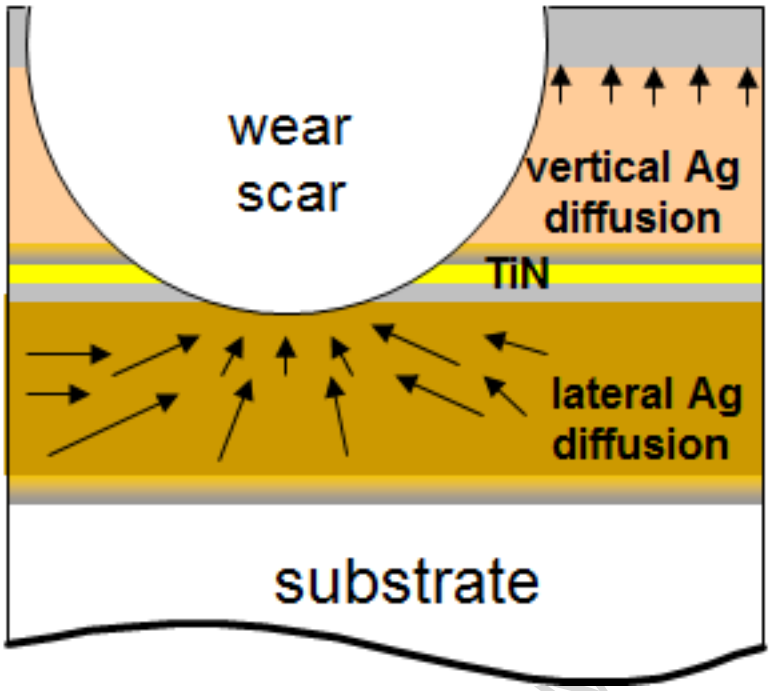

Figure 4a

Submitted for publication in Surface and Coatings Technology

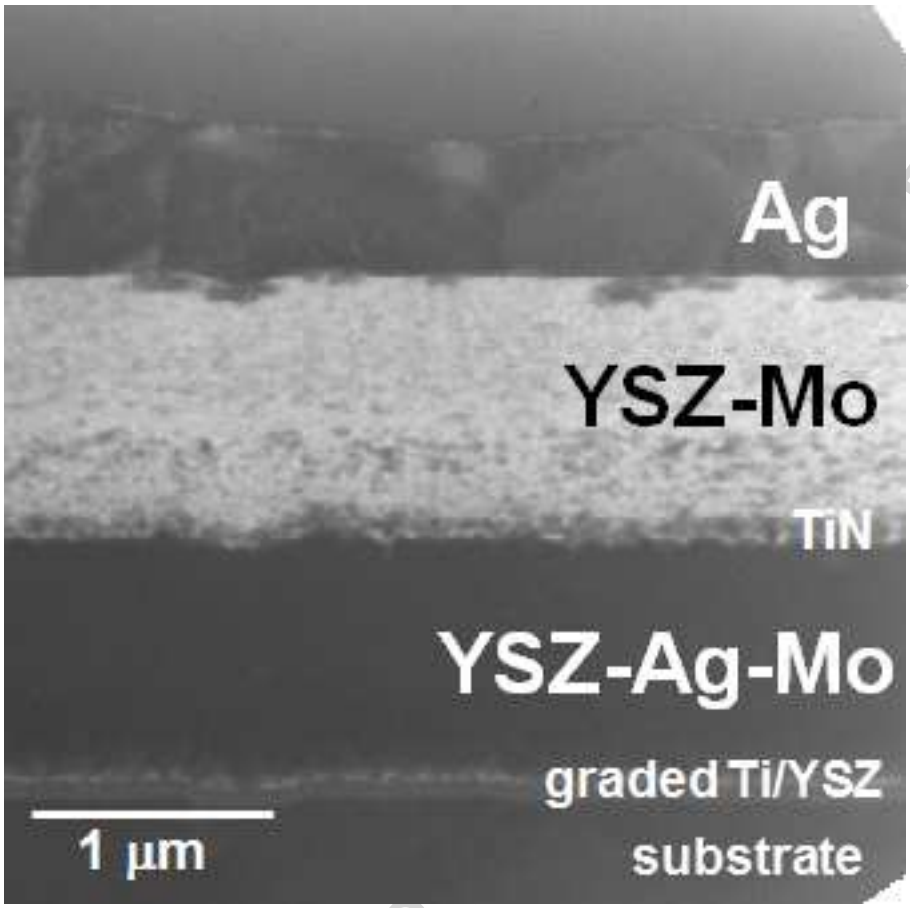

Figure 4b

Submitted for publication in Surface and Coatings Technology

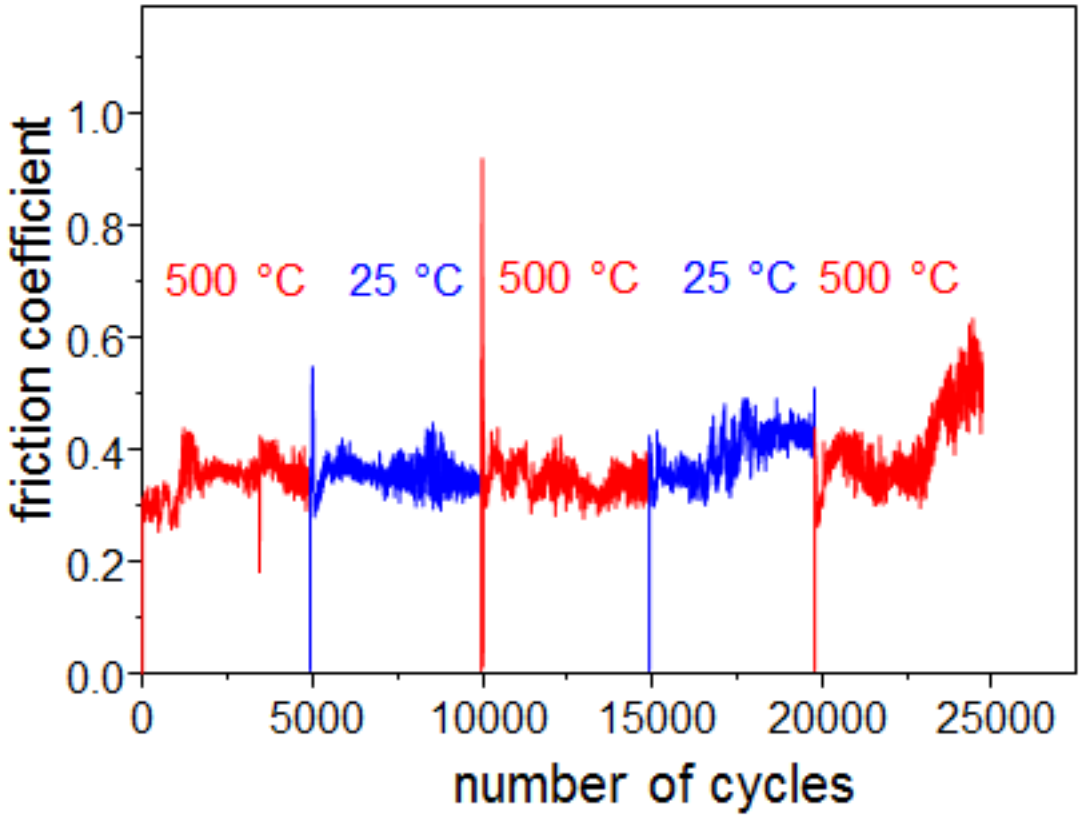

Figure 4c

Submitted for publication in Surface and Coatings Technology

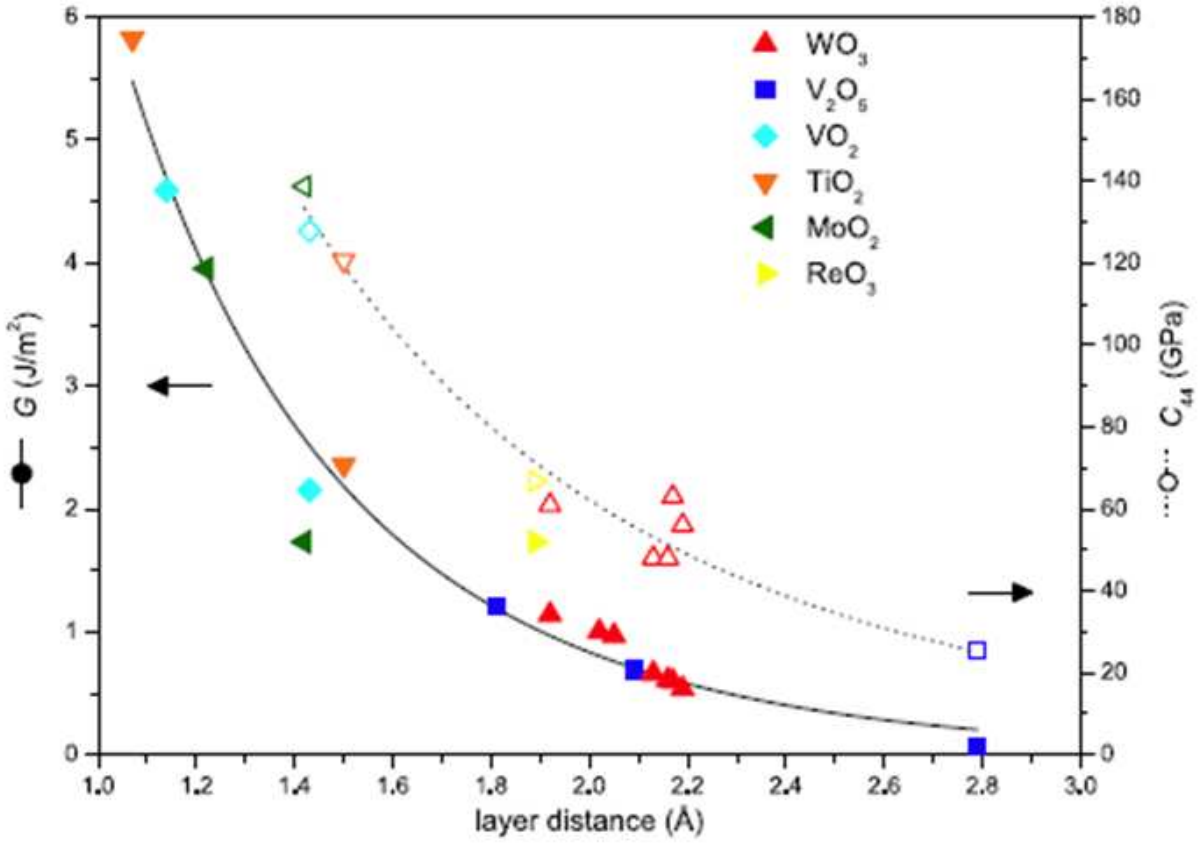

Figure 5a

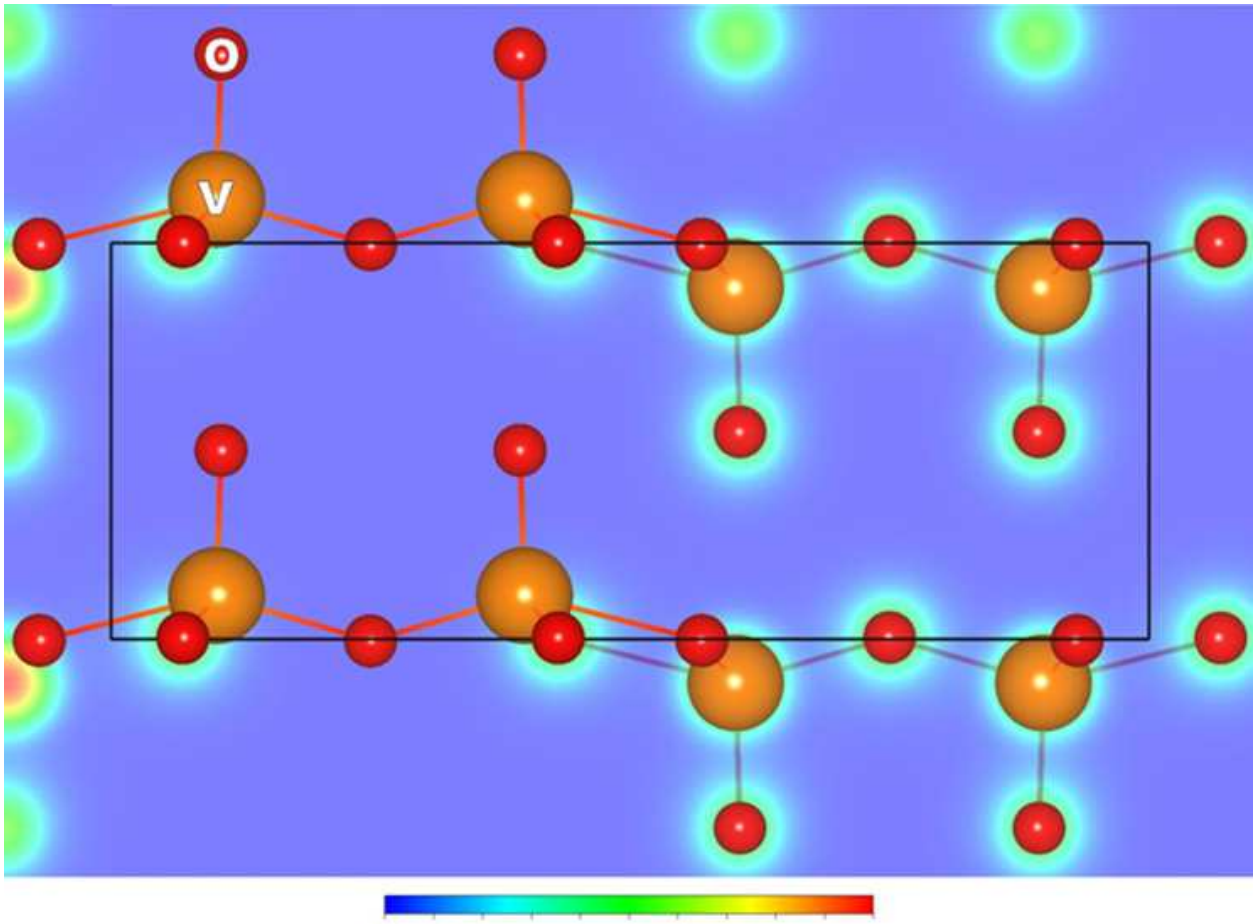

Figure 5b

Submitted for publication in Surface and Coatings Technology

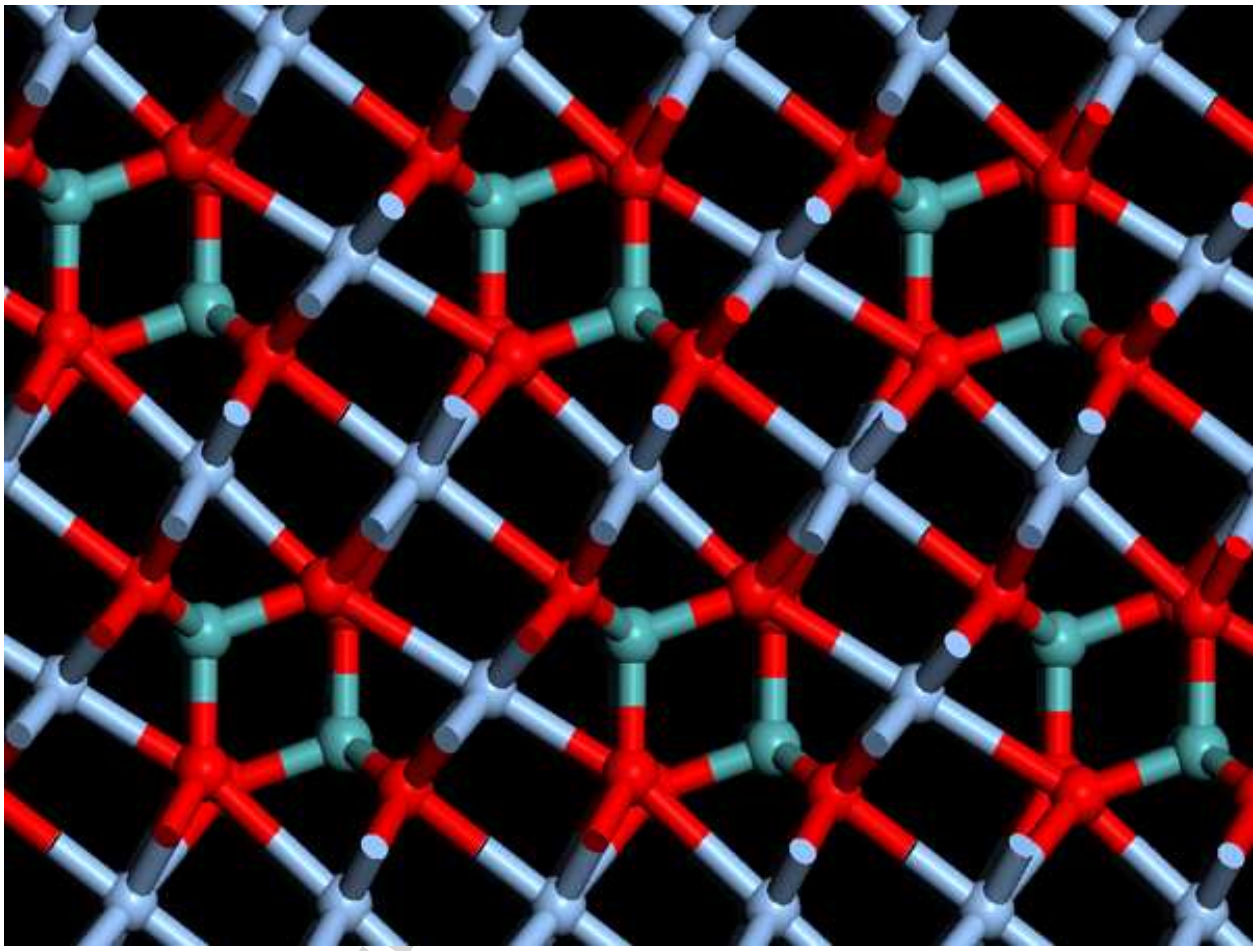

Figure 6a

Submitted for publication in Surface and Coatings Technology

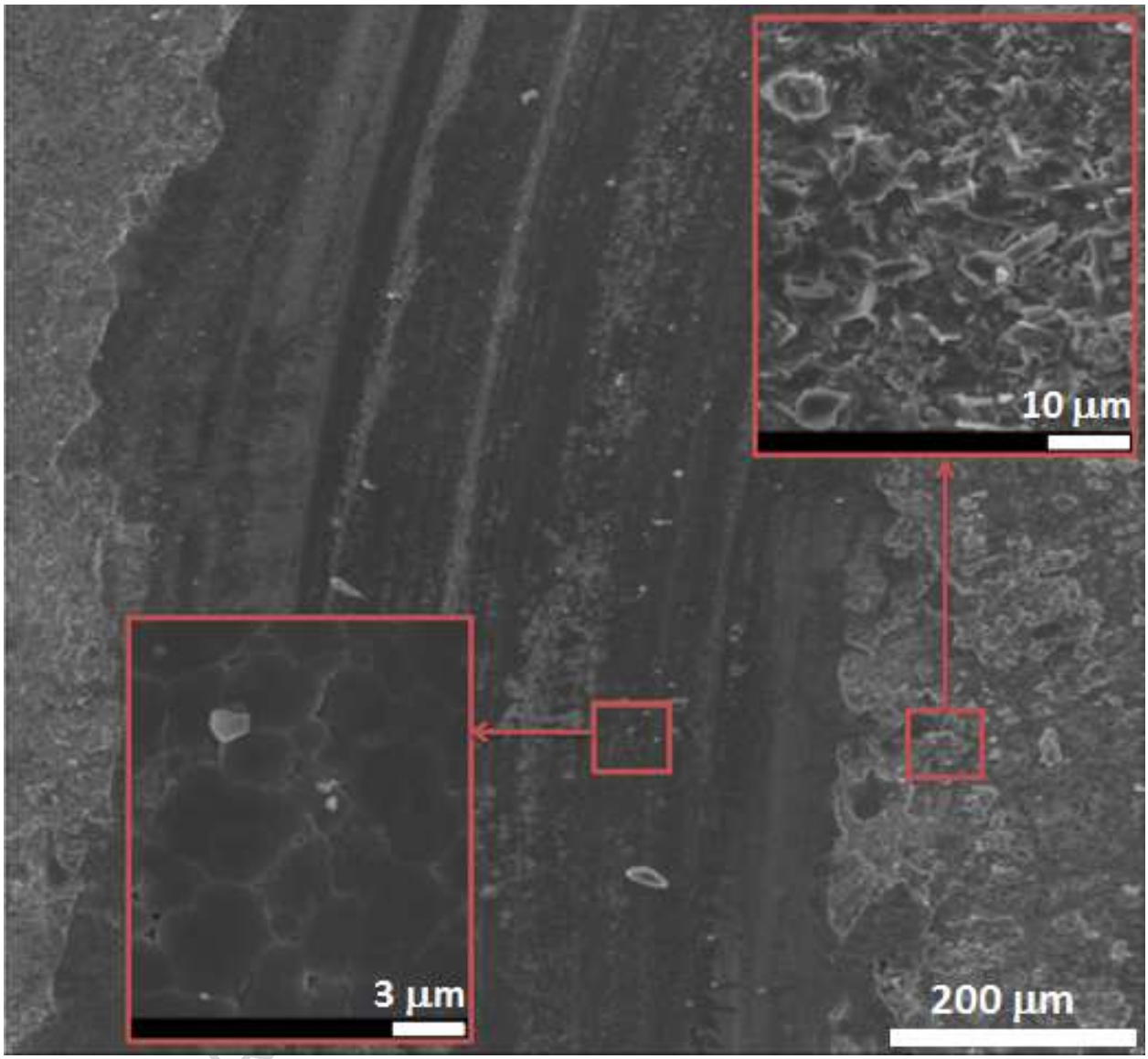

Figure 6b

Submitted for publication in Surface and Coatings Technology

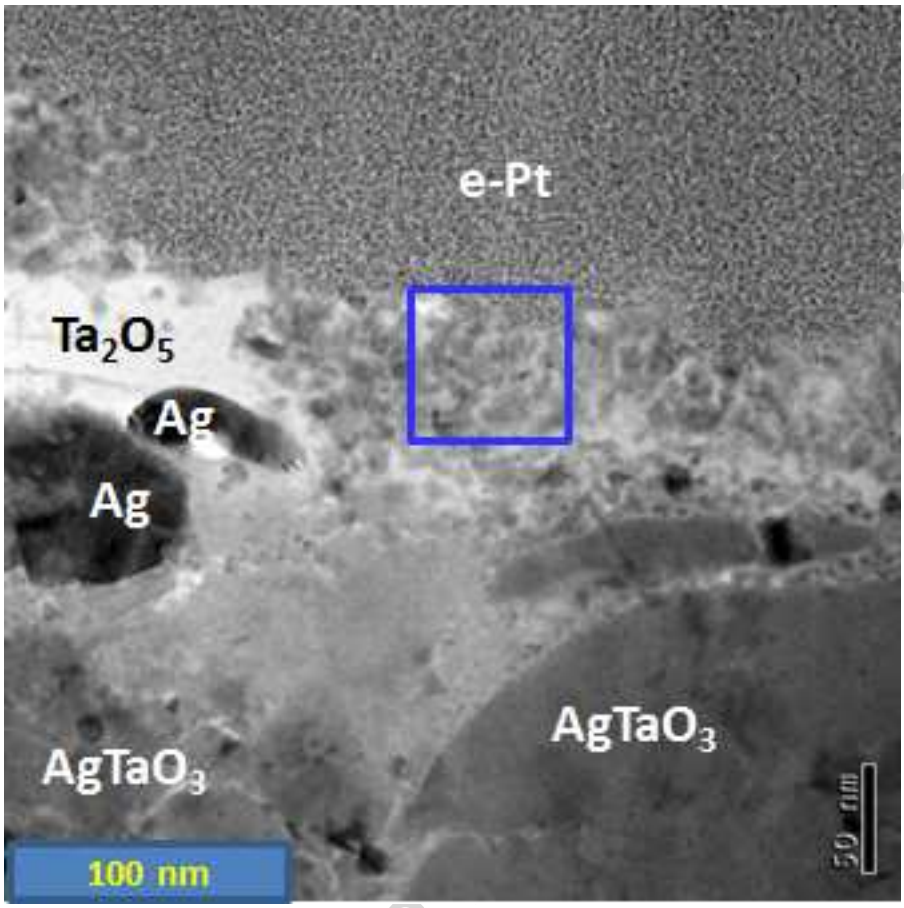

Figure 7a

Submitted for publication in Surface and Coatings Technology

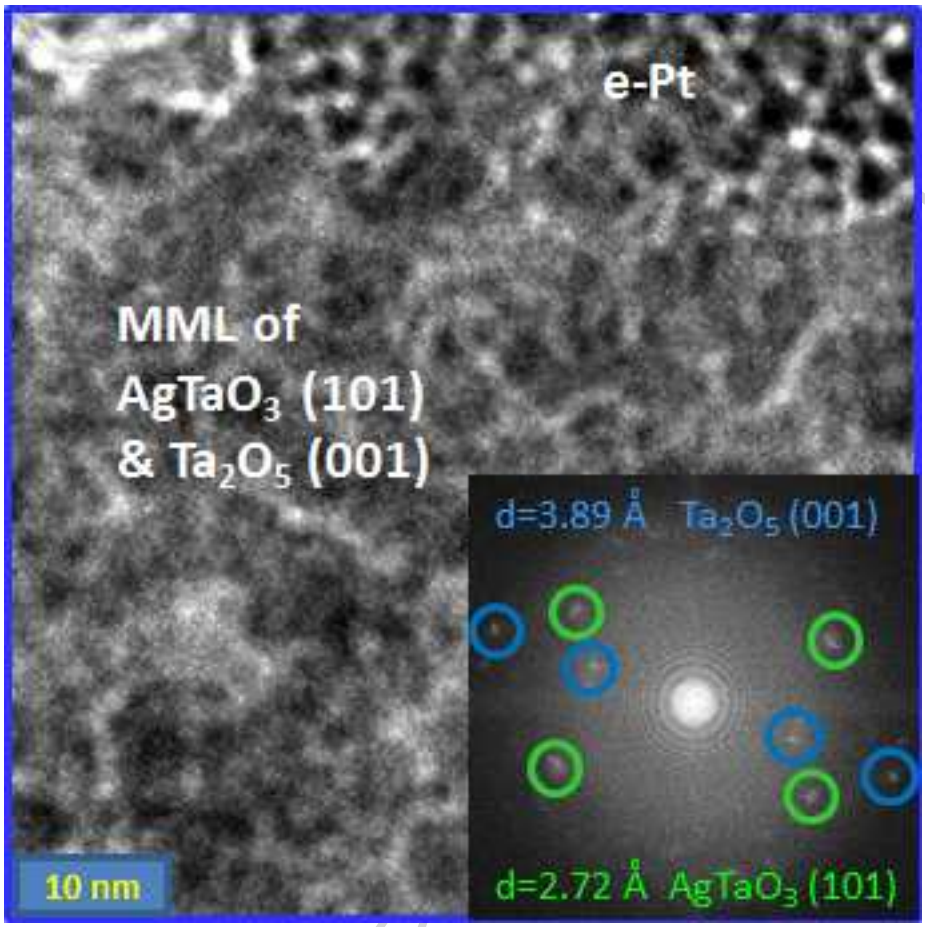

Figure 7b

Submitted for publication in Surface and Coatings Technology

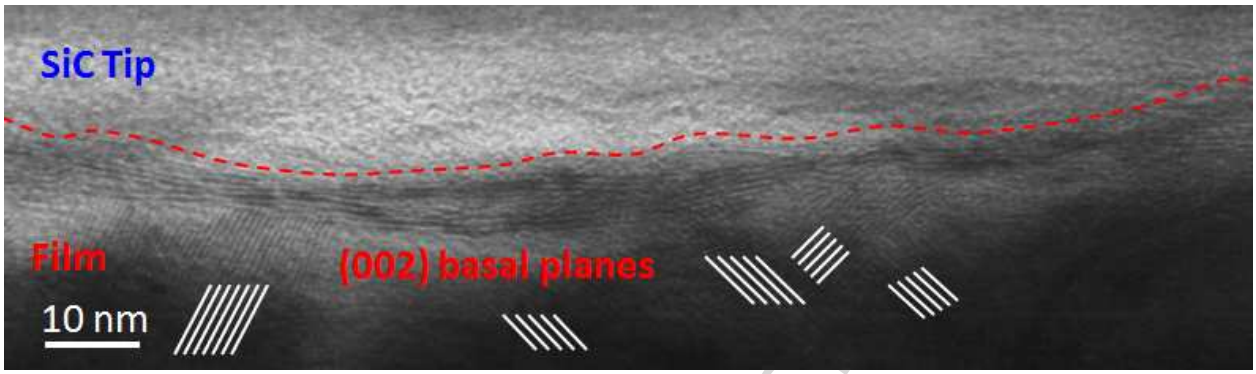

Figure 8

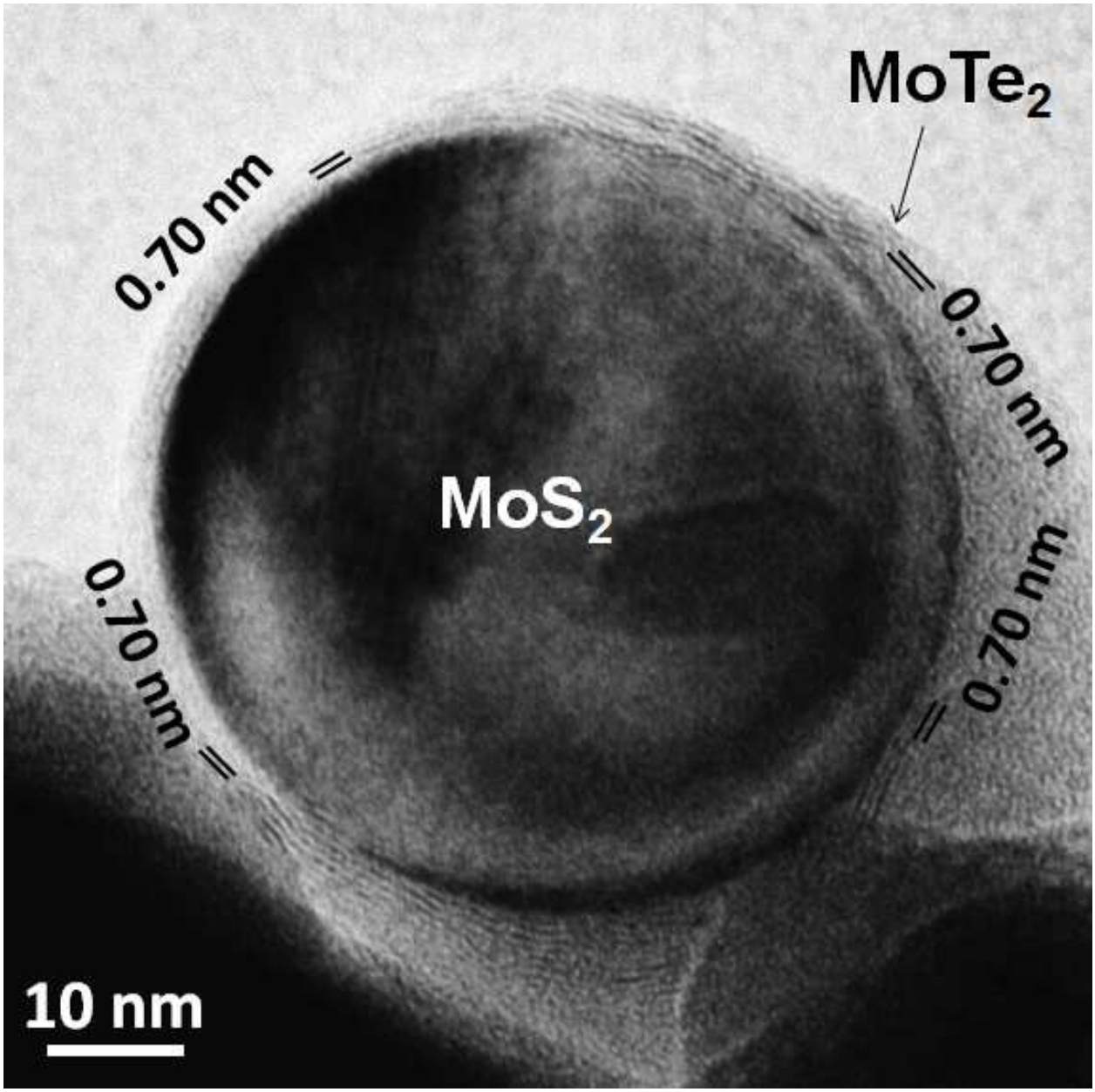

Figure 9a

Submitted for publication in Surface and Coatings Technology

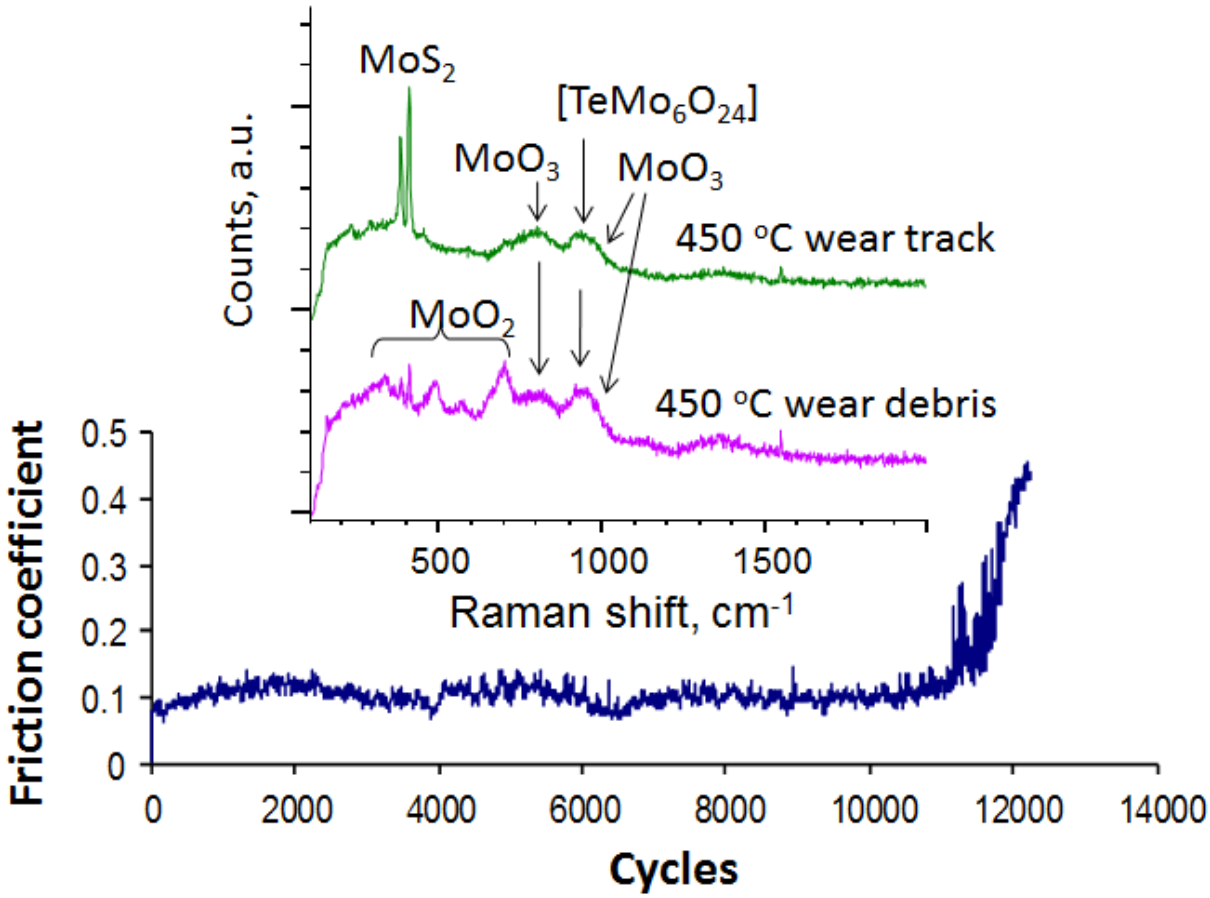

Figure 9b

Submitted for publication in Surface and Coatings Technology

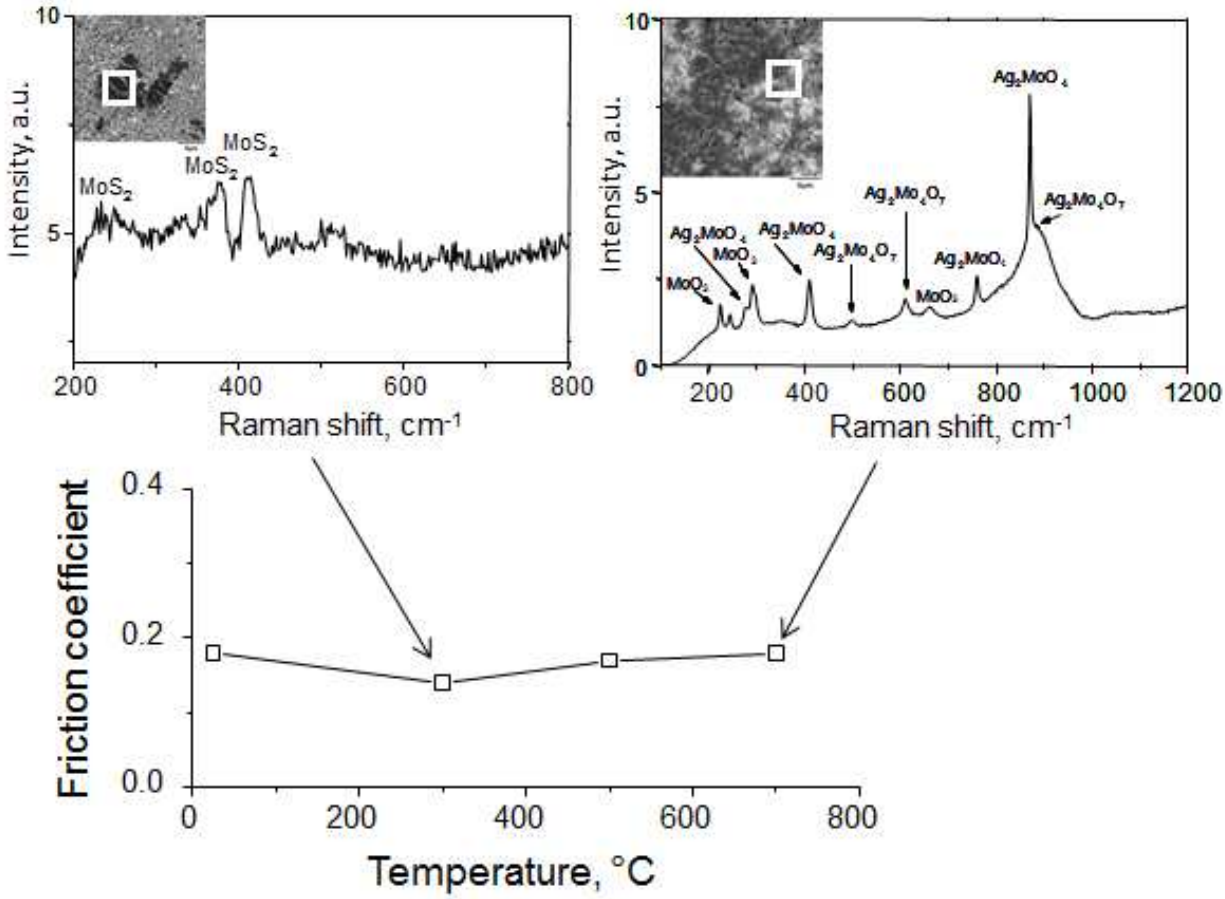

Figure 10

Submitted for publication in Surface and Coatings Technology

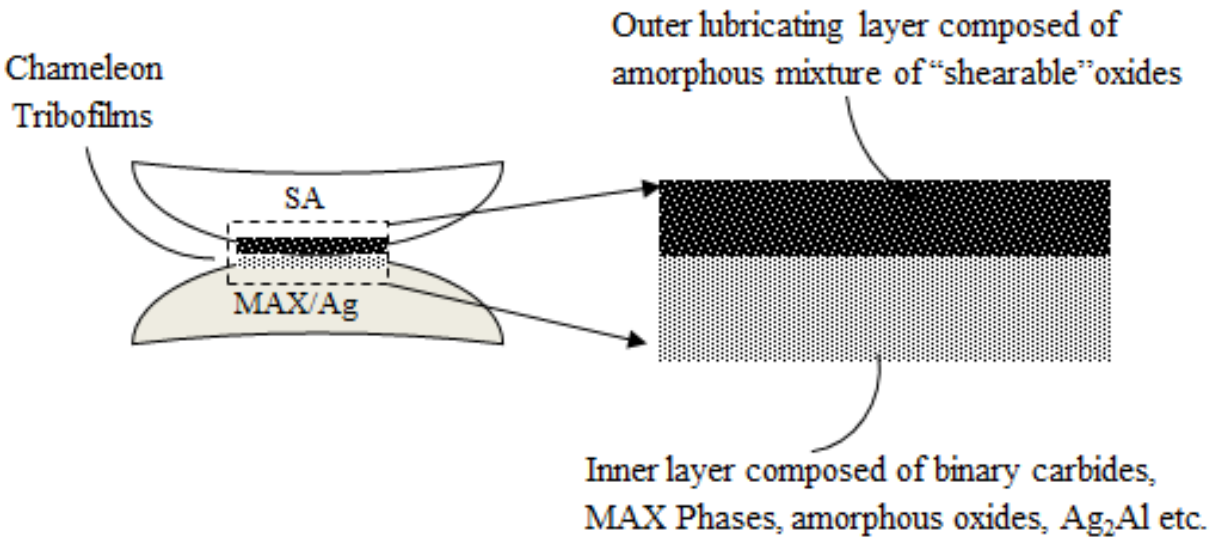

Figure 11a

Submitted for publication in Surface and Coatings Technology

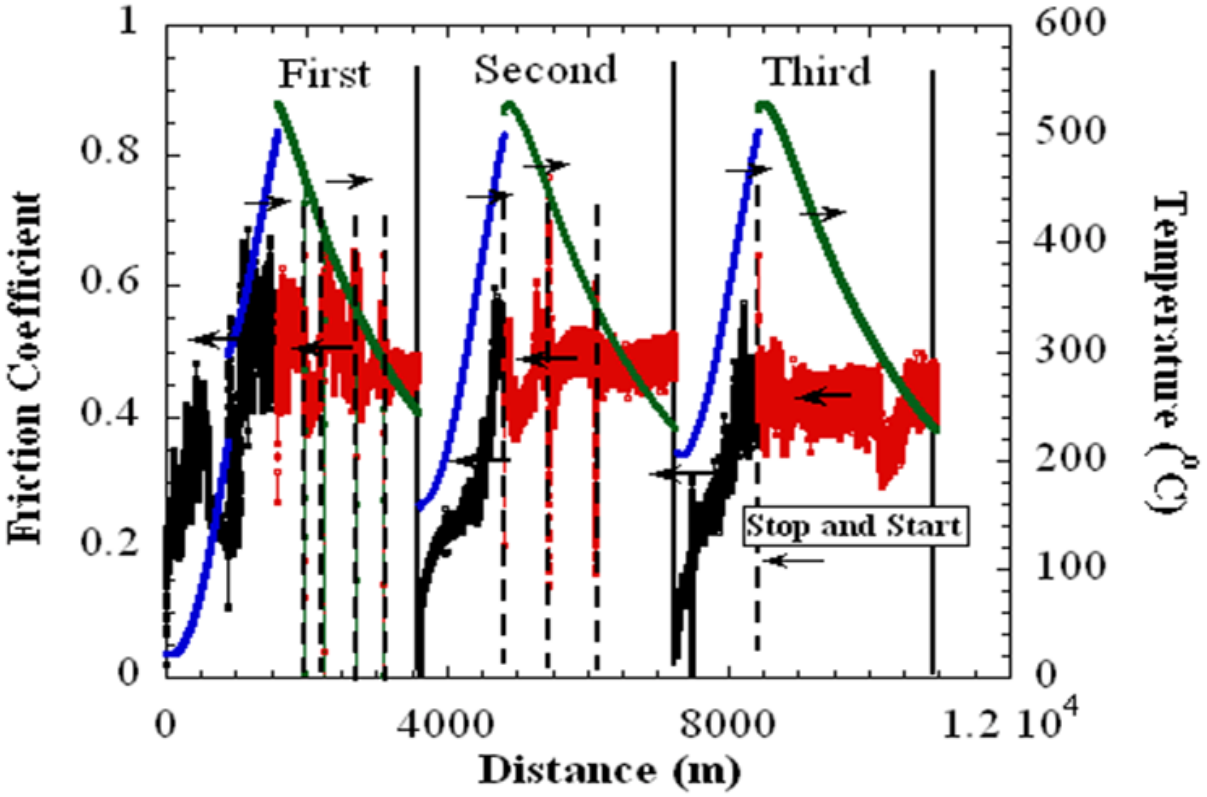

Figure 11b

Submitted for publication in Surface and Coatings Technology

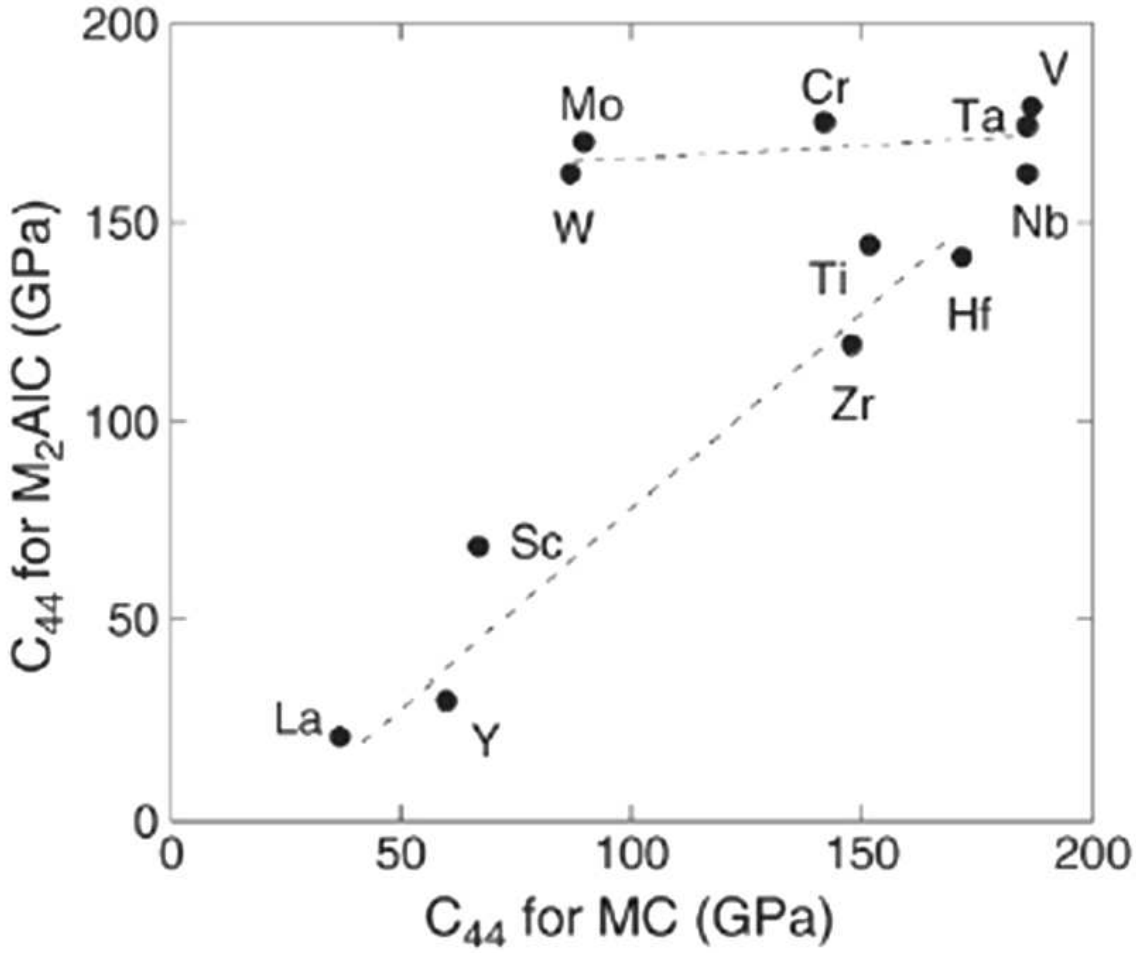

Figure 12a

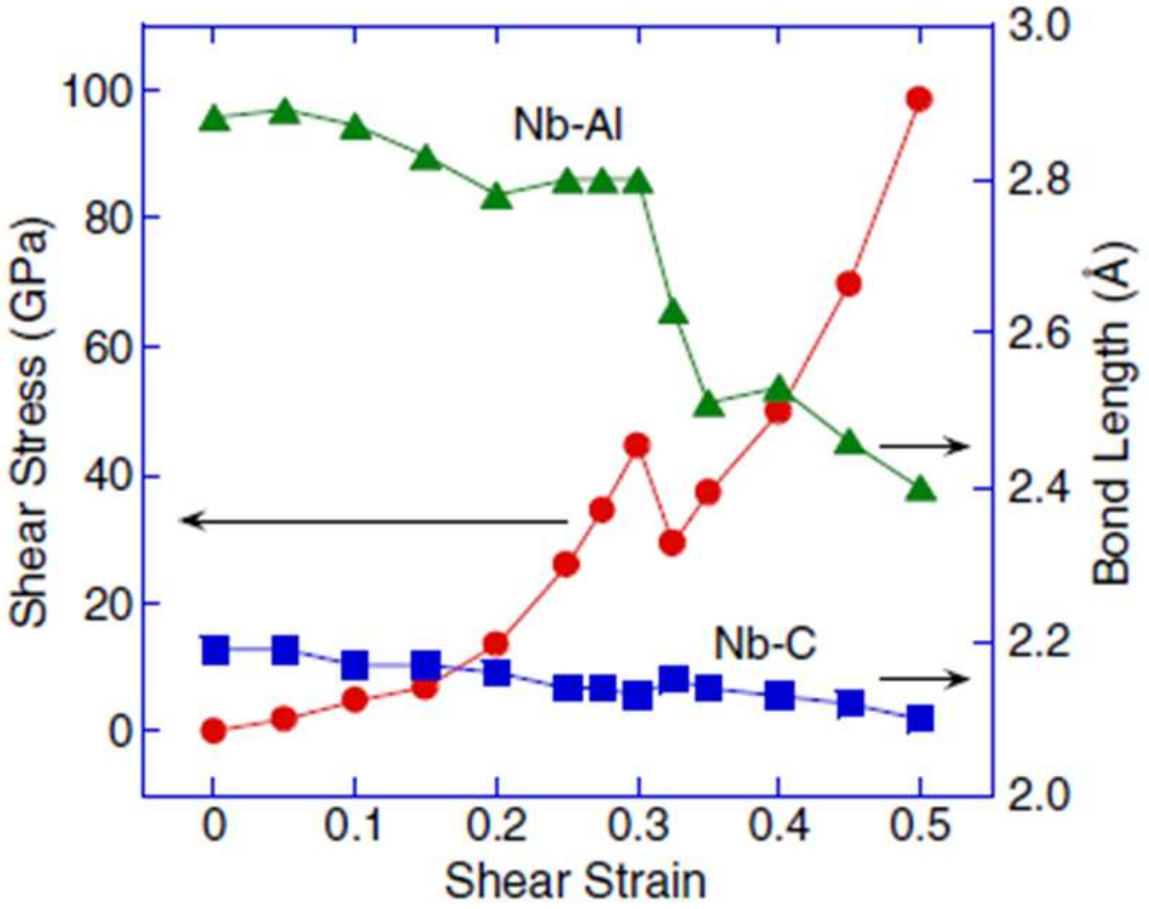

Figure 12b

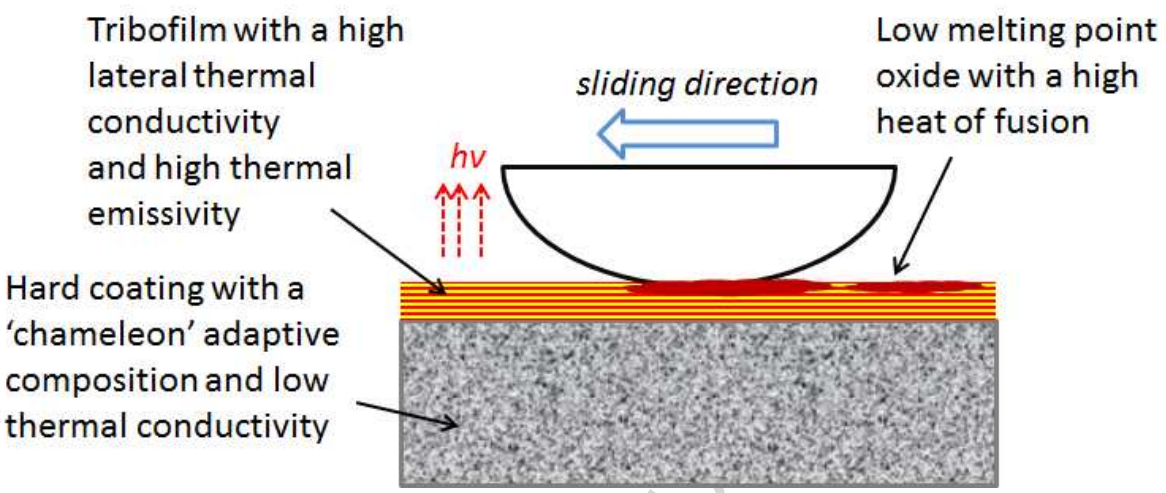

Figure 13

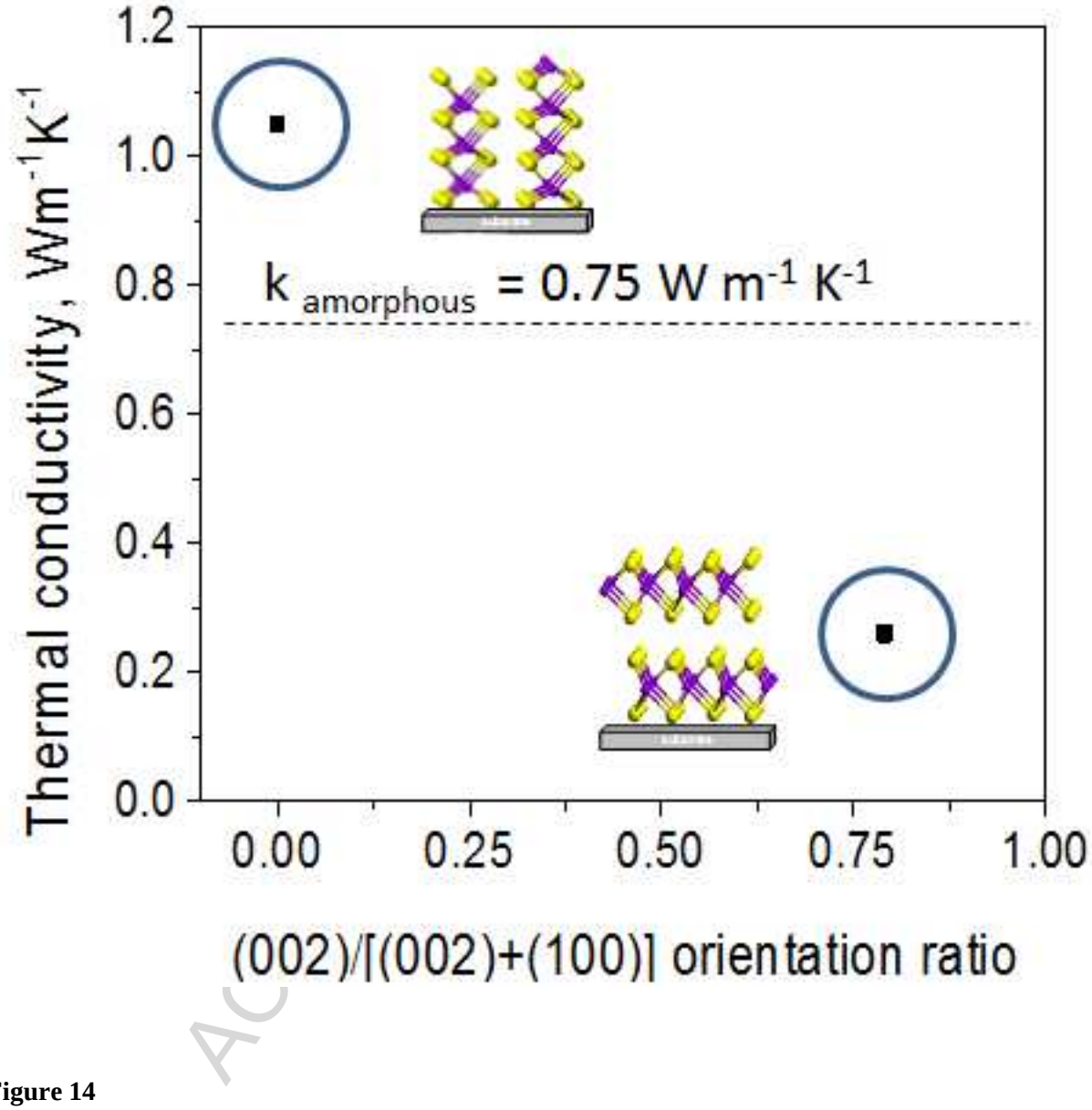
Thermal conductivity, $Wm^{-1}K^{-1}$
1.2
1.0
0.8
0.6
0.4
0.2
0.0
$k_{amorphous}$ = 0.75 W m^{-1} K^{-1}
0.00
0.25
0.50
0.75
1.00
(002)/[(002)+(100)] orientation ratio

Figure 14

Submitted for publication in Surface and Coatings Technology

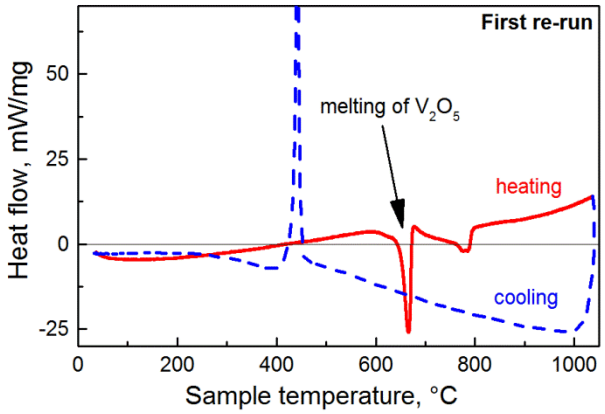

Figure 15

Submitted for publication in Surface and Coatings Technology

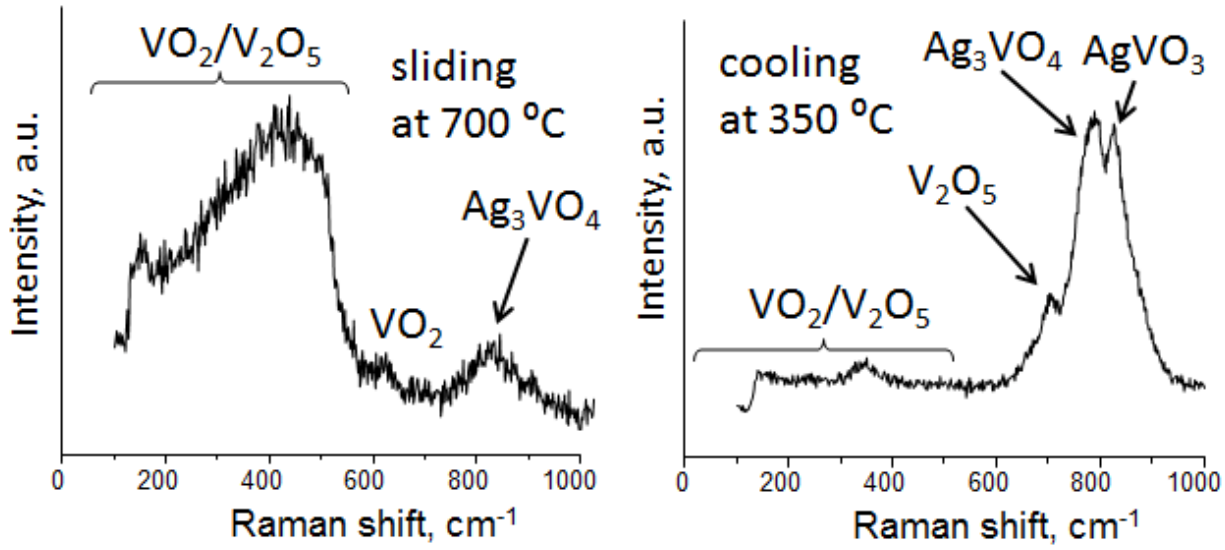

Figure 16a

Submitted for publication in Surface and Coatings Technology

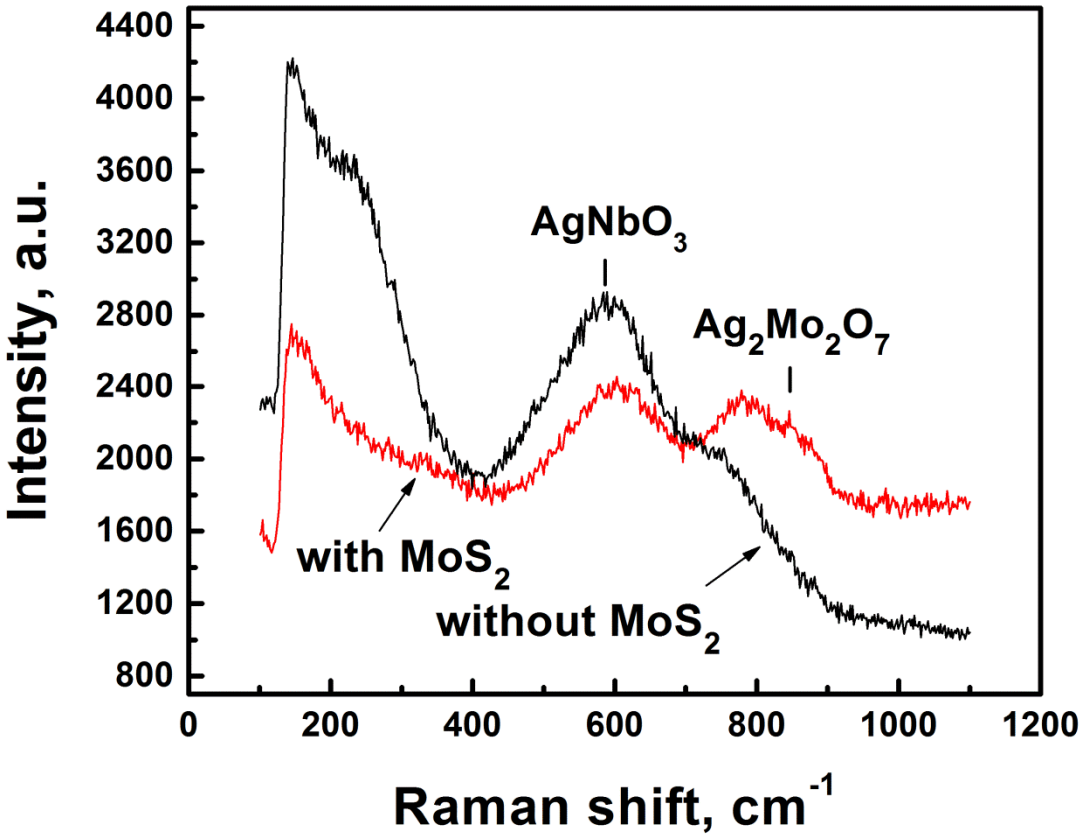

Figure 16b

Submitted for publication in Surface and Coatings Technology

Table 1. Comparison of currently most typically used high temperature solid lubrication adaptive mechanisms.

Adaptive Mechanism	**Typical Temperature Range (in air)**	**Material Examples**	**Benefits**	**Challenges**
Structural transitions with hexagonal solid basal plane formation	<300 °C	MoS_2 , WS_2, Graphite DLC ($sp^3 \rightarrow sp^2$) a-C, a-C:H with metal carbides and nitrides MoS_2-Sb_2O_3-graphite MoS_2-Sb_2O_3 MoS_2-WSe_2 MoS_2 encapsulated in oxides and nitrides	-Lowest friction and wear rates -Low cost options (burnishing)	Oxidation at higher temperatures
Diffusion of soft metals to contact surface	300-500 °C	Ag and Au encapsulated in ZrO_2, Al_2O_3, TiN, CrN, VN, TaN, Mo_2N, NbN	-Oxidation stable -Temperature self-regulated	Fast diffusion to surface depletes metal lubricant reservoirs
Lubricious oxide formation at contact surface	500-1000 °C	Magnéli phases: - V_2O_5, MoO_3, TiO_2, - WO_3, PbO, ZnO Double oxides: -silver molybdates, -silver vanadates -silver niobates -silver tantalates Silicate glass forming: - Cs_2MoOS_3 - Cs_2WOS_3	-Provides liquid lubrication – very low friction -Environment supplies oxygen -Wear track self-healing -Some (glasses) use counterpart to form lubricant	Abrasion at low temperatures Lubricant extrusion from contact by the load